ventricular myocytes.[3–5] During development, HCN channels are abundantly expressed in the embryonic ventricle, but their expression progressively declines after birth, and is restricted to the conduction system in healthy adult hearts.[6] However, HCN channels, especially HCN2 and HCN4, are re-expressed in hypertrophied and failing hearts in both rodents and humans, and the resultant increase in $I_f$ currents in ventricular myocytes is thought to provide an important trigger that initiates clinically significant arrhythmias in those hearts.[3–7] Direct evidence showing the contribution of induced ventricular expression of HCN channels to enhanced myocardial arrhythmicity in vivo is lacking, however. Nor has blockade of HCN channel been shown to prevent malignant arrhythmias or sudden death associated with heart failure independently of heart rate reduction.

We recently reported that a transcriptional repressor, neuron-restrictive silencer factor (NRSF, also named REST) is an important regulator of the fetal cardiac gene program.[8] Transgenic mice that selectively express a dominant-negative form of NRSF (dnNRSF) in their hearts (dnNRSF-Tg) develop progressive cardiomyopathy leading to sudden arrhythmic death beginning at about 8 weeks of age.[9] Hearts from dnNRSF-Tg mice show increased expression of fetal type ion channel genes, including *HCN2* and *HCN4*, which is consistent with what has been observed in other animal models of heart disease and in human failing hearts.[6,7,10,11] Moreover, $I_f$ amplitude was correspondingly increased in ventricular myocytes from dnNRSF-Tg hearts, which raises the possibility that $I_f$ currents in some way contribute to the occurrence of arrhythmias in dnNRSF-Tg hearts.[9]

To clarify the contribution made by HCN channels to the development of arrhythmias associated with heart failure, and to assess the capacity of HCN channel blockade to prevent malignant arrhythmias, in the present study we tested the effects of ivabradine, a HCN channel blocker, on survival and ventricular arrhythmicity in dnNRSF-Tg mice. We also generated and analyzed transgenic mice overexpressing HCN2 channel in a cardiac specific manner (HCN2-Tg). Our findings demonstrate that increased expression of HCN channels contributes to the increased arrhythmicity observed in failing hearts.

## Methods

### Animal Experiments

Beginning at 8 weeks of age, dnNRSF-Tg mice and control wild-type (WT) littermates were left untreated (control) or were treated with ivabradine (7 mg/kg per day orally) given in drinking water ad libitum. The dose of ivabradine, which minimally affected heart rate in dnNRSF-Tg mice, was chosen based to earlier reports and our preliminary studies.[12,13] We adjusted the concentration of ivabradine dissolved in the water based on the water consumption among each group. Ivabradine was supplied by Servier Laboratories.

A mouse HCN2 cDNA was cloned into the SalI site of pBluescript IIKS(+) plasmid containing the α-myosin heavy chain (MHC) promoter. The resultant α-MHC-HCN2 transgenic construct was then released from the vector backbone by digestion with NotI and purified for injection into the pronucleus of fertilized oocytes harvested from C57BL/6J mice. The surviving embryos were then transferred to the oviducts of pseudopregnant MCH mice. Using an osmotic minipump (Alzet osmotic pumps, Durect Corp) according to the manufacture's protocol, isoproterenol (15 mg/kg per day) or vehicle was subcutaneously administered for 7 days, beginning at 23 weeks of age. The animal care and all experimental protocols were reviewed and approved by the Animal Research Committee at Kyoto University Graduate School of Medicine.

### Patch Clamp Studies

Ventricular myocytes were dispersed as reported previously, and perfused with the physiological bathing solution during the experiment.[9,14] The physiological bathing solution contained (in mmol/L); 140 NaCl, 5.4 KCl, 0.5 $MgCl_2$, 1.8 $CaCl_2$, 5 HEPES (pH=7.4 with NaOH). We used Axopatch200B amplifier and Digidata 1320 interface (Axon Instruments, Inc.) for the electrophysiological measurements. The patch pipettes were filled with high K solution containing; 100 K-Aspartate, 30 KCl, 5 $Na_2$-creatine phosphate, 5 $K_2ATP$, 1 $MgCl_2$, 5 EGTA, 5 HEPES (pH=7.2 with KOH). We recorded action potential with perforated patch method (0.3 mg/mL amphotericin in high K solution), and $I_f$ current with ruptured patch method. A stock solution of 10 mmol/L ivabradine in dimethyl sulfoxide was diluted to the desired concentration using $Na^+$-free bathing solution (final concentration, 3 μmol/L). Since the onset of ivabradine effect is relatively slow, we evaluated the effect of ivabradine during the second minute after addition of ivabradine.[15]

### Intracardiac Electrophysiology

Mice were intubated and anesthetized with 0.5% to 1.5% isoflurane, after which surface electrocardiography leads (limb leads) were placed. Then, using a 1.7 French octapolar catheter (CIBer mouse EP, NuMe, Hopkinton) inserted via the jugular vein, a standard electrophysiological study protocol was performed as described previously.[9,16] Rapid ventricular pacing using the extrastimulation ($S_1S_2$) technique was carried out using 2 to 3 extra stimuli to determine the ventricular refractory period and to attempt induction of ventricular arrhythmias. The stimulation was administered at twice the ventricular diastolic capture threshold.

## Noninvasive Blood Pressure and Heart Rate Measurements

Systolic blood pressure (SBP) and heart rate (HR) were measured in conscious mice using the tail-cuff method (Softron Co Ltd) as described previously,[9] unless otherwise indicated.

## Echocardiographic and Hemodynamic Analysis

Echocardiography was performed using an echocardiography system (Toshiba power vision 8000, Toshiba Corp) equipped with a 12-MHz imaging transducer as described previously.[9] Hemodynamic parameters assessed by catheter in WT mice and dnNRSF-Tg mice were obtained as described previously[9]

## Histological Examination

Hearts were fixed in 10% formalin and prepared for histological analysis as described previously.[9]

## Quantitative RT-PCR Analysis

Using 50 ng of total RNA prepared from ventricles, levels of mouse *ANP*, *BNP*, *SERCA2*, *CACNA1H*, *HCN2*, *HCN4*, *Col1a1*, *Col3a1*, *FN1*, *MMP2*, *MMP9*, and *Tgfb1* and *GAPDH* mRNA were determined by quantitative real-time PCR using the manufacture's protocol (Applied Biosystems, Inc) as previously described.[9,17] The primers and the probe sets were purchased from Applied Biosystems.[9,17]

## Ambulatory Electrocardiography

To monitor ambulatory electrocardiographs, radio frequency transmitters (TA 10ETA-F20; Data Science) were implanted as previously described.[9]

## Heart Rate Variability

Fifteen-minute periods of electrocardiographic data with little noise and few ectopic beats were collected 3 to 5 days after implantation of radio frequency transmitters and then analyzed for heart rate variability (HRV). Because of its circadian rhythm, 4 HRV data sets collected during periods extending from 7:00 to 12:00, 13:00 to 18:00, 19:00 to 24:00, and 1:00 to 6:00 hours were averaged for each mouse. Spectral analysis of the heart rate recordings using a fast Fourier transform (FFT) algorithm on sequences of 1024 points was carried out using HEM 3.4 software (Notocord). Cut-off frequencies for power in the low-frequency (LF: 0.15 to 1.5 Hz) and high-frequency (HF: 1.5 to 5.0 Hz) ranges were based on previous experiments with mice.[18] After FFT analysis, the data that contained ectopic beats or arrhythmic events were deleted manually. In mice, HRV predominantly correlates with parasympathetic activity.[18]

## Statistical Analysis

Survival of dnNRSF-Tg mice treated with and without ivabradine was monitored for 24 weeks, beginning when the mice were 8 weeks of age. During that period, the numbers of mice that died were recorded, and the survival data were analyzed using the Kaplan–Meier method with the log-rank test (the outcome was death). We also used nonparametric analyses to evaluate percentage of $I_f$ currents, heart rate, blood pressure, body weight, heart weight-body weight ratio, lung weight-body weight ratio, hemodynamic parameters, numbers of arrhythmias, numbers of action potentials, water consumption, percentage of collagen area, cardiac gene expression, HRV, and resting membrane potentials. In our analysis of unpaired data using nonparametric tests, the compared groups and conditions were as follows: numbers of arrhythmias in control untreated versus ivabradine-treated dnNRSF-Tg mice and in WT versus HCN2-Tg mice; numbers of action potentials induced by isoproterenol in isolated ventricular myocytes from dnNRSF-Tg mice treated with vehicle versus ivabradine; the percentage of collagen area in WT versus HCN2-Tg mice; water consumption by isoproterenol-treated WT versus HCN2-Tg mice; cardiac gene expression in WT versus HCN2-Tg mice; heart rate, blood pressure, body weight, heart weight-body weight ratio, and lung weight-body weight ratio in WT versus HCN2-Tg mice; and hemodynamic parameters in untreated WT versus untreated HCN2-Tg and in isoproterenol-treated WT versus isoproterenol-treated HCN2-Tg. Comparisons between 2 unpaired groups were made using the Mann–Whitney test. In our analysis of paired data using nonparametric tests, the compared groups and conditions were as follows: the percentage of $I_f$ currents in isolated ventricular myocytes from dnNRSF-Tg and HCN2-Tg mice recorded in the absence versus presence of ivabradine and the numbers of action potentials induced by isoproterenol in ventricular myocytes isolated from HCN2-Tg mice in the absence versus presence of ivabradine. Comparisons between 2 paired groups were made using the Wilcoxon signed-rank test. Comparisons were also made among multiple (more than 2) groups using nonparametric tests. These included: heart rates, blood pressures, body weights, heart weight-body weight ratios, lung weight-body weight ratios, hemodynamic parameters, and water consumption among untreated WT, ivabradine-treated WT, untreated dnNRSF-Tg, and ivabradine-treated dnNRSF-Tg; the percentage of collagen area among untreated WT, untreated dnNRSF-Tg, and ivabradine-treated dnNRSF-Tg; cardiac gene expression among untreated WT, ivabradine-treated WT, untreated dnNRSF-Tg,

and ivabradine-treated dnNRSF-Tg; HRV among untreated WT, untreated dnNRSF-Tg, and ivabradine-treated dnNRSF-Tg; resting membrane potentials among untreated WT, untreated dnNRSF-Tg, and ivabradine-treated dnNRSF-Tg; and heart rates, blood pressures and heart weight-body weight ratios among control vehicle-treated WT, isoproterenol-treated WT, vehicle-treated HCN2-Tg, and isoproterenol-treated HCN2-Tg. Comparisons among multiple groups were made using Kruskal-Wallis nonparametric analysis of variance (ANOVA) followed by the Bonferroni correction. Values of $P<0.05$ were considered significant in the experiments other than those analyzed using Kruskal–Wallis nonparametric ANOVA followed by the Bonferroni correction, in which $P<0.0166$ and $P<0.00833$ were considered significant for comparisons among 3 and 4 groups, respectively. Data analyzed by using nonparametric tests are presented as box plots or dot plots.

## Results

### Specific HCN Channel Blocker Ivabradine Improves Survival Among dnNRSF-Tg Mice

We previously showed that dnNRSF-Tg mice develop progressive cardiomyopathy and begin to die from ventricular tachyarrhythmias at about 8 weeks of age.[9] In dnNRSF-Tg hearts, *HCN2* and *HCN4*, 2 genes encoding HCN channels and transcriptional targets of NRSF/REST, were upregulated, and there was a corresponding increase in $I_f$ amplitude in the isolated ventricular myocytes. By contrast, no stable $I_f$ currents were recorded in adult ventricular myocytes from the WT littermates' hearts.[9] To determine the role played by HCN channels in the development of malignant arrhythmias and sudden death, and to assess the potential therapeutic effect of HCN channel blockade in dnNRSF-Tg mice, we administered ivabradine, a specific HCN channel blocker, beginning when the mice were 8 weeks of age. Initially, we confirmed that ivabradine significantly blocked $I_f$ currents in ventricular myocytes from dnNRSF-Tg mice (Figure 1A and 1B). In Figure 1A, we applied 3 $\mu$mol/L ivabradine, which is close to the half maximal inhibitory concentration ($IC_{50}$) for all HCN channels.[19] Although at a dose of 7 mg/kg per day, ivabradine reduced heart rate in WT mice, it did not significantly affect heart rate in dnNRSF-Tg mice, whose basal heart rates were slower than those of WT mice (Figure 1C and Table 1). Despite having no effect on heart rate, ivabradine significantly improved the survival rate among dnNRSF-Tg mice (Figure 1D). Blood pressures, body weights, heart-to-body weight ratios, and lung-to-body weight ratios did not differ between the control and ivabradine groups in either genotype (Table 1 and Figure 1E through 1G). On the other hand, heart-to-body weight ratios were significantly higher in dnNRSF-Tg mice than WT mice, as described previously.[9] At a dose of 7 mg/kg per day, ivabradine did not affect water consumption in either genotype, which is consistent with an earlier report (Figure 2A).[12] Echocardiographic and histological parameters, including the percentage of fibrosis area, showed no significant differences between untreated and ivabradine-treated dnNRSF-Tg mice (Table 1 and Figure 2B and 2C). Likewise, hemodynamic parameters measured during cardiac catheterization did not significantly differ between the 2 groups of dnNRSF-Tg mice (Table 1). By contrast, echocardiography and cardiac catheterization showed that, as compared to untreated WT mice, left ventricular systolic function was disturbed and the percentage of fibrotic area was significantly increased in untreated dnNRSF-Tg mice, as described previously (Figure 2C and Table 1).[9] Consistent with those findings, there was no significant difference in the expression of the cardiac stress marker genes *ANP*, *BNP*, and *SERCA2* between the untreated and ivabradine-treated groups within either genotype, whereas the expression of these genes differed between untreated WT mice and untreated dnNRSF-Tg mice as described previously (Figure 3A through 3C).[9,20,21] Moreover, the mRNA expression levels of *HCN2* and *HCN4*, as well as *CACNA1H*, which encodes the T-type calcium channel, did not differ between untreated and ivabradine-treated mice within either genotype (Figure 3D through 3F). The ventricular expression levels of *HCN2*, *HCN4*, and *CACNA1H* mRNA were higher in dnNRSF-Tg mice than WT mice as described previously (Figure 3D through 3F).[9] Expression of the fibrosis-related genes collagen type1 $\alpha$1 (*Col1a1*), collagen type3 $\alpha$ 1 (*Col3a1*), fibronectin 1 (*FN1*), matrix metallopeptidase 2 (*MMP2*), matrix metallopeptidase 9 (*MMP9*), and transforming growth factor-$\beta$ 1 (*Tgfb1*) did not differ between WT and dnNRSF-Tg mice and was not affected by ivabradine treatment in either genotype (Figure 4A through 4F). All of these data suggest that ivabradine directly suppresses sudden death in dnNRSF-Tg mice without affecting heart rate or cardiac structure or function.

### Ivabradine Suppresses Arrhythmicity in dnNRSF-Tg Mice

We next used a telemetric monitoring system to examine the effects of ivabradine on electrocardiographic parameters in dnNRSF-Tg mice. We found that ivabradine tended to suppress the number of premature ventricular contractions (PVCs) in dnNRSF-Tg hearts (Figure 5A). More importantly, it dramatically reduced the number of episodes of ventricular tachycardia (VT) (Figure 5B). To elucidate the mechanism by which ivabradine suppressed arrhythmias in dnNRSF-Tg mice, we evaluated its effect on arrhythmogenic re-entrant substrates by carrying out an in vivo intracardiac electrophysiological analysis in dnNRSF-Tg mice.[9,16] We found that

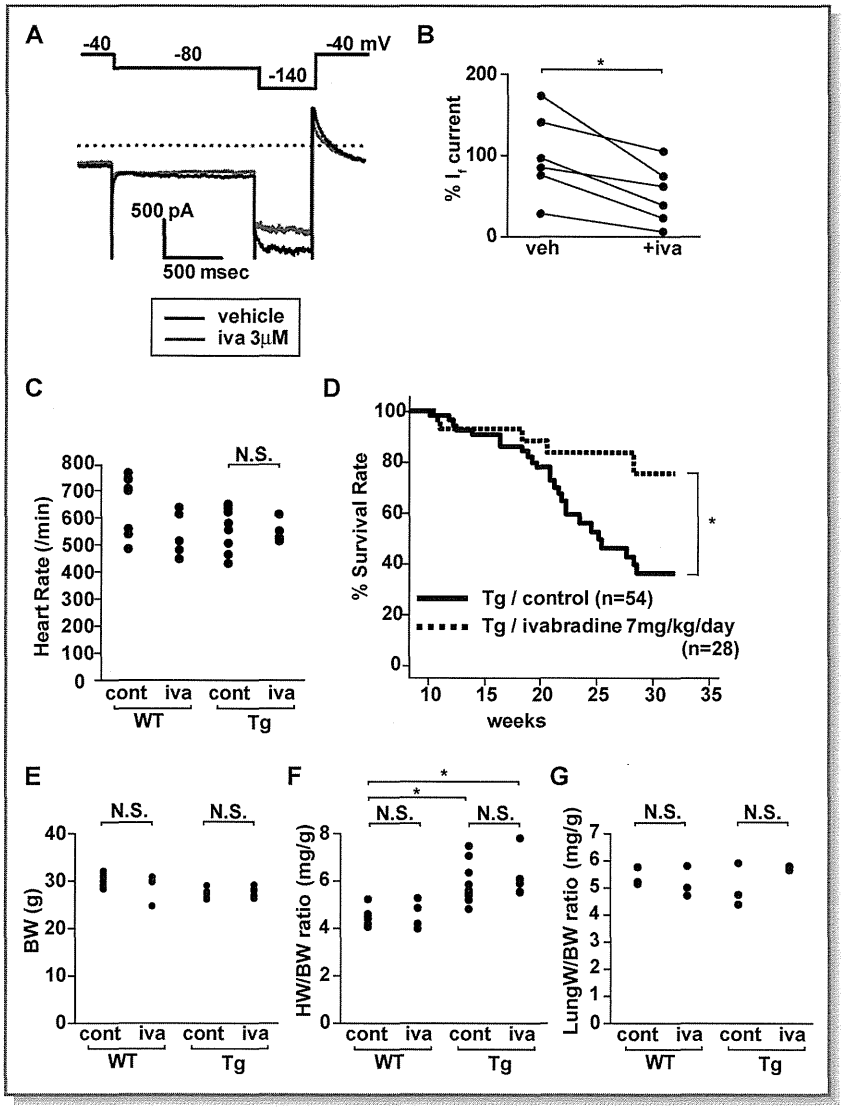


**Figure 1.** Ivabradine (iva) prolongs survival among dnNRSF-Tg (Tg) mice. A, Representative $I_f$ currents recorded in ventricular myocytes from a Tg mouse in the presence (red line; 2 minutes after the application of iva) and absence of iva (black line). Inward-rectifier $K^+$ current was suppressed by 0.5 mmol/L $BaCl_2$. Pulse protocol is shown in the top. B, Relative $I_f$ amplitudes (%) measured at −140 mV in the absence (vehicle, indicated as veh) and presence of iva (+iva). A mean relative $I_f$ amplitudes (%) in the absence of iva was assigned a value of 100 (n=6 each). **P*<0.05 vs vehicle. The Wilcoxon signed-rank test was used for the analysis. C, Heart rates in wild-type (WT) and Tg mice at 20 weeks of age, with and without 12 weeks of iva treatment (n=9 for untreated control WT, n=5 for WT with iva, n=10 for untreated control Tg and n=6 for Tg with iva). Kruskal–Wallis nonparametric ANOVA followed by the Bonferroni correction was used for analysis among the 4 groups. NS, not significant. Graphs are shown in dot plots. D, Kaplan–Meyer survival curves for Tg mice, with or without ivabradine. Drug treatment began when the mice were 8 weeks of age and lasted 24 weeks: **P*<0.05 (n=54 for Tg without drugs [control], 28 for Tg with ivabradine). E through G, Body weights (BW) (E), heart weight-to-body weight ratios (HW/BW) (F) and lung-to-body weight ratios (LW/BW) (G) in 20-week-old WT and Tg mice, with or without iva (for BW and HW/BW comparisons, n=9 for untreated WT, n=4 for WT treated with iva, n=11 for untreated Tg, and n=6 for Tg treated with iva; for LW/BW comparisons, n=3 in each group). Kruskal–Wallis nonparametric ANOVA followed by the Bonferroni correction was used for analysis among the 4 groups. **P*<0.00833. NS, not significant. Data in E through G are shown as dot plots. dnNRSF-Tg indicates dominant-negative form of neuron-restrictive silencer factor transgenic mice; ANOVA, analysis of variance; cont, control.

dnNRSF-Tg mice were highly susceptible to induction of VT, as reported previously[9] (Figure 5C), and that ivabradine did not reduce their susceptibility (Figure 5C), indicating that ivabradine does not modulate the arrhythmogenic re-entrant substrates observed in dnNRSF-Tg ventricles. We also assessed the effect of ivabradine on autonomic nerve activity by analyzing HRV, as imbalanced autonomic nerve activity can trigger ventricular arrhythmias in failing hearts.[22,23] As we

**Table 1.** Hemodynamic Parameters in 20-Week-Old WT and dnNRSF-Tg Mice Treated With or Without Ivabradine

| | WT | | dnNRSF-Tg | |
|---|---|---|---|---|
| | Control | Iva | Control | Iva |
| Blood pressure, mm Hg | 105.1±3.7 | 100.4±6.6 | 100.2±1.1 | 98.3±3.5 |
| Heart rate, /min | 671±36.6 | 541±37.7 | 576±25.8 | 550±15.1 |
| Echocardiographic data | | | | |
| LVDd, mm | 3.3±0.18 | 3.13±0.19 | 4.11±0.14* | 4.04±0.08* |
| LVDs, mm | 1.65±0.13 | 1.4±0.12 | 2.87±0.13* | 2.67±0.06* |
| IVST, mm | 0.89±0.03 | 0.83±0.04 | 0.77±0.03 | 0.76±0.03 |
| PWT, mm | 0.93±0.04 | 0.87±0.03 | 0.82±0.04 | 0.79±0.04 |
| FS, % | 50.3±1.8 | 54.0±1.2 | 30.5±1.2* | 33.6±1.3* |
| Hemodynamic data | | | | |
| LVSP, mm Hg | 102.9±1.9 | 101.0±0.2 | 92.6±1.1 | 93.1±1.9 |
| LVEDP, mm Hg | 4.0±1.1 | 4.9±1.3 | 6.4±1.4 | 6.0±1.0 |
| dP/dt, mm Hg/s | 11 729.6±200.5 | 11 779.6±462.8 | 5754.7±626.5 | 6580.3±445.6 |
| −dP/dt, mm Hg/s | 5429.5±179.0 | 5584.1±462.8 | 4306.0±227.0 | 4500.8±474.6 |

Values are means±SEM. Numbers of mice tested for blood pressure and heart rate are 9 for untreated control WT, 5 for WT with ivabradine, 10 for untreated dnNRSF-Tg, and 6 for dnNRSF-Tg with ivabradine. Numbers of mice tested for echocardiography are 8 for untreated control WT, 3 for WT with ivabradine, 14 for untreated dnNRSF-Tg, and 13 for dnNRSF-Tg with ivabradine. Numbers of mice tested for hemodynamic analysis are 3 for each group. Kruskal–Wallis nonparametric ANOVA followed by the Bonferroni correction was used for analysis among the 4 groups. WT indicates wild type; dnNRSF-Tg, dominant-negative form of neuron-restrictive silencer factor transgenic mice; Control, untreated control mice; Iva, mice treated with ivabradine; LVDd, left ventricular diastolic dimension; LVDs, left ventricular systolic dimension; IVST, interventricular septum thickness; PWT, posterior wall thickness; FS, fractional shortening; LVSP, left ventricular systolic pressure; LVEDP, left ventricular end diastolic pressure; dP/dt, first derivative of pressure; ANOVA, analysis of variance.
*$P<0.00833$ vs untreated wild type.

previously reported,[21] HRV was diminished in dnNRSF-Tg mice, and was unaffected by ivabradine (Figure 5D). All of these results indicate that ivabradine suppresses malignant arrhythmias without affecting re-entrant substrates or autonomic imbalance in dnNRSF-Tg mice. This suggests ivabradine acts directly to suppress abnormal impulse formation caused by abnormally enhanced automaticity or triggered activity.

## Ivabradine Reduces the Frequency of Spontaneous Action Potential in Cardiac Ventricular Myocytes From dnNRSF-Tg Mice

We also evaluated the effects of ivabradine on the abnormal impulse formation seen in ventricular myocytes from dnNRSF-Tg mice. We first examined the effects of long-term treatment with ivabradine on the electrophysiological properties of myocytes isolated from dnNRSF-Tg hearts. As we showed previously,[14] the resting membrane potential was somewhat depolarized in ventricular myocytes isolated from dnNRSF-Tg hearts, as compared to WT hearts, which was largely attributed to the decrease in density of inward-rectifier $K^+$ current.[24] Ivabradine did not significantly affect the resting membrane potential in dnNRSF-Tg myocytes (Figure 5E).

We previously reported that in the presence of isoproterenol, ventricular myocytes isolated from dnNRSF-Tg hearts showed early after-depolarizations and spontaneous action potentials, but myocytes from WT hearts did not, demonstrating the higher susceptibility of dnNRSF-Tg myocytes to β-adrenergically–induced arrhythmias.[9,24] Moreover, it is known that increasing cyclic adenosine monophosphate (cAMP) levels through β-adrenergic stimulation causes $I_f$ currents to become faster and larger in amplitude than the currents elicited under unstimulated conditions.[2,6] We therefore assessed the effect of ivabradine on the response of dnNRSF-Tg myocytes to β-adrenergic stimulation. In dnNRSF-Tg ventricular myocytes exposed to isoproterenol, ivabradine tended to reduce the occurrence of spontaneous action potentials (Figure 5F and 5G), which supports our idea that increased ventricular expression of HCN channels leads to an abnormal increase in automaticity that contributes to arrhythmogenesis in dnNRSF-Tg mice.

## Increased Expression of HCN2 in Ventricular Myocytes Promotes Susceptibility to Arrhythmias Induced by Chronic Isoproterenol Treatment

To further assess the role of induced HCN channel expression in increased cardiac arrythmicity, we generated transgenic mice exhibiting specific cardiac expression of HCN2 driven by the α-MHC promoter (HCN2-Tg) (Figure 6A). In HCN2-Tg mice,

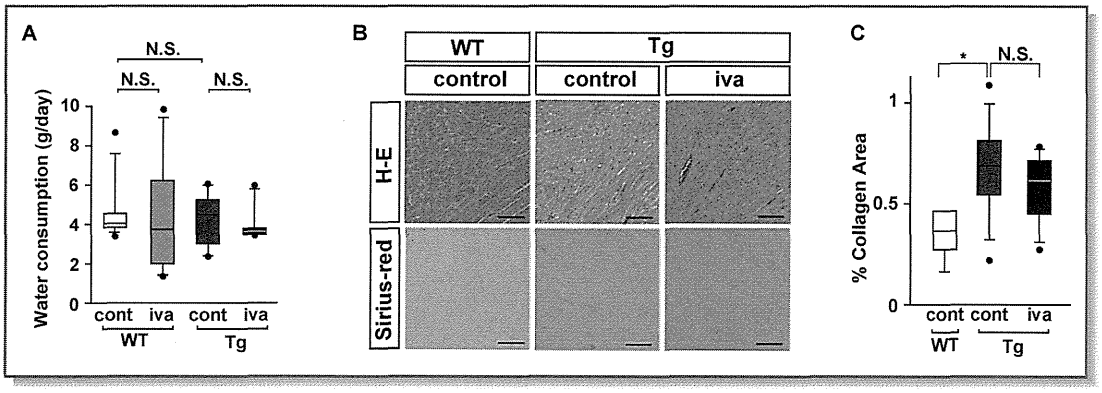


**Figure 2.** Effects of ivabradine (iva) on the water consumption and histology in dnNRSF-Tg (Tg) mice. A, Water consumption (g/day) in 12-week-old WT and Tg mice, with or without iva (n=8 for untreated [cont] WT mice, n=6 for WT mice treated with iva, n=6 for untreated (cont) Tg mice, n=6 for Tg mice treated with iva). Kruskal–Wallis nonparametric ANOVA followed by the Bonferroni correction was used for analysis among the 4 groups. B, Histology of WT and Tg hearts from 20-week-old mice treated with or without iva: H-E, Hematoxylin-Eosin staining; scale bars, 100 $\mu$m. C, Graphs show the percentage of collagen area in untreated (cont) WT mice, Tg mice treated without (cont) or with iva (n=5 for untreated WT mice, n=9 for untreated Tg mice, n=7 for Tg mice treated with iva). Kruskal–Wallis nonparametric ANOVA followed by the Bonferroni correction was used for the analysis among the 3 groups. *$P$<0.0166. All data are shown as box plots. NS indicates not significant; WT, wild type; cont, control; dnNRSF-Tg, dominant-negative form of neuron-restrictive silencer factor transgenic mice; ANOVA, analysis of variance.

ventricular HCN2 mRNA levels were significantly higher than in their WT littermates (Figure 6B), whereas ventricular HCN4 mRNA levels were similar in the 2 genotypes (Figure 6C). In addition, HCN2-Tg mice showed a 50-fold increase in the expression of HCN2 protein, as compared to WT mice (Figure 6D). We also confirmed the presence of $I_f$ currents in ventricular myocytes from HCN2-Tg mice, and that they were inhibited by 3 $\mu$mol/L ivabradine (Figure 6E through

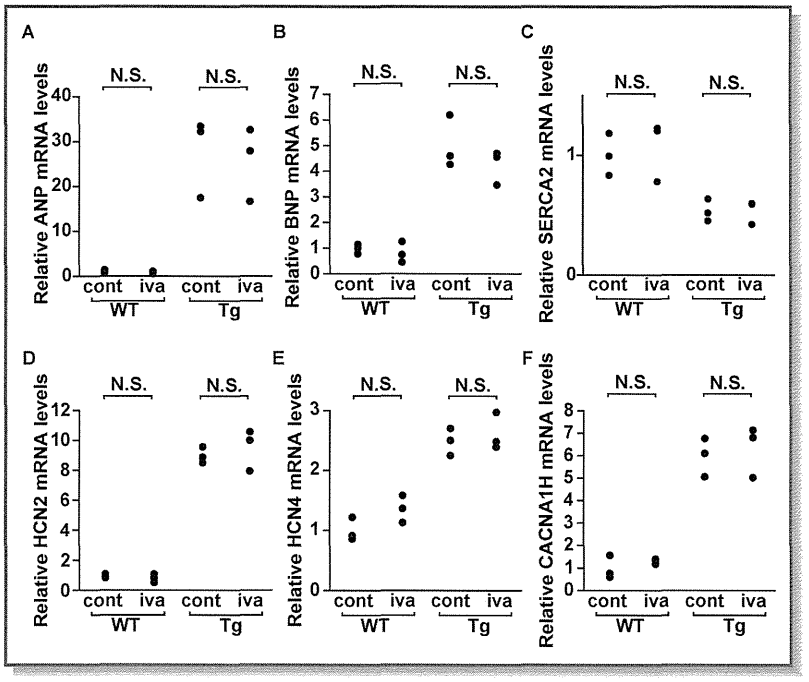


**Figure 3.** Effects of ivabradine (iva) on the gene expression in dnNRSF-Tg (Tg) mice. A through F, Relative levels of *ANP* (A), *BNP* (B), *SERCA2* (C), *HCN2* (D), *HCN4* (E), and *CACNA1H* (F) mRNA in hearts from 20-week-old WT and Tg mice treated with or without iva. n=3 in each group. Mice treated without iva are indicated as cont. Kruskal–Wallis nonparametric ANOVA followed by the Bonferroni correction was used for analysis among the 4 groups. All data are shown as dot plots. NS indicates not significant; ANP, atrial natriuretic peptide; cont, control; WT, wild type; dnNRSF-Tg, dominant-negative form of neuron-restrictive silencer factor in transgenic mice; BNP, brain natriuretic peptide; SERCA2, sarcoplasmic/endoplasmic reticulum calcium ATPase 2; HCN2, hyperpolarization-activated cyclic nucleotide-gated channel 2; CACNA1H, calcium channel, voltage-dependent, T type, alpha 1H subunit; ANOVA, analysis of variance.

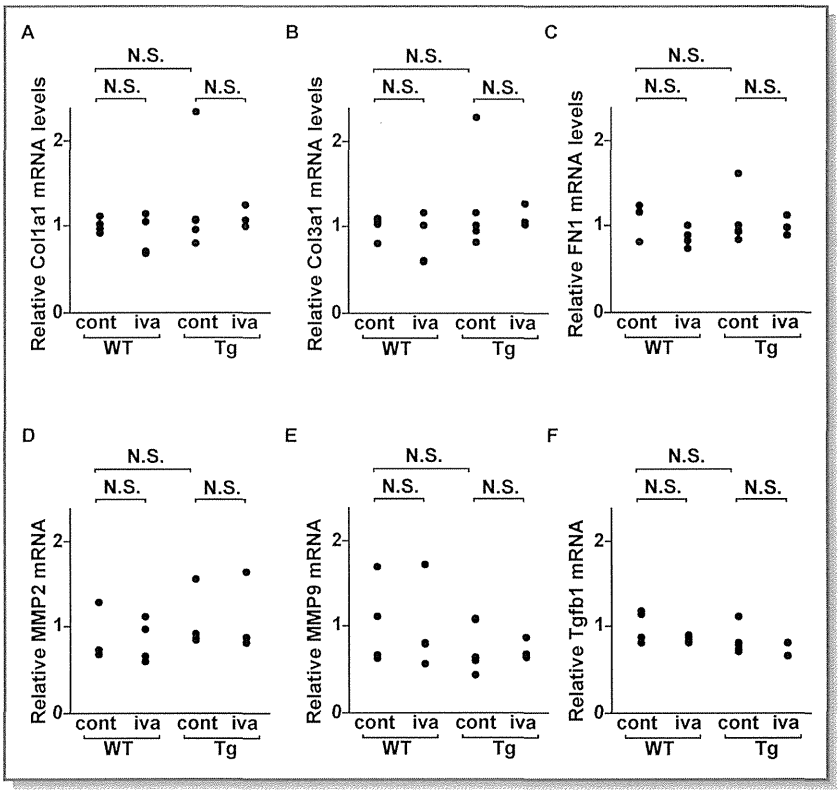


**Figure 4.** Effects of ivabradine (iva) on the fibrosis-related genes expression in dnNRSF-Tg (Tg) mice. A through F, Relative levels of *Col1a1* (A), *Col3a1* (B), *FN1* (C), *MMP2* (D), *MMP9* (E), and *Tgfb1* (F) mRNA in hearts from 20-week-old WT and Tg mice treated with or without iva. n=4 for WT without iva, n=4 for WT with iva, n=5 for Tg without iva, and n=3 for Tg with iva. Mice treated without iva are indicated as cont. Kruskal–Wallis nonparametric ANOVA followed by the Bonferroni correction was used for the analysis. All data are shown as dot plots. NS indicates not significant; dnNRSF-Tg, dominant-negative form of neuron-restrictive silencer factor transgenic mice; ANOVA, analysis of variance; WT, wild type; cont, control; Col1a1, collagen type1 α1; Col3a1, collagen type3 α 1; FN1, fibronectin 1; MMP2, matrix metallopeptidase 2, MMP9, matrix metallopeptidase 9; Tgfb1, transforming growth factor- β 1.

6H). By contrast, $I_f$ currents were not detected in ventricular myocytes from the WT littermates (data not shown), as reported previously.[9] The amplitudes of $I_f$ currents in HCN2-Tg ventricular myocytes were ≈1.5 times larger than in dnNRSF-Tg myocytes (Figure 6F). [9]

HNC2-Tg mice raised under normal conditions were viable and fertile, and their body weights, heart-to-body weight ratios, and lung-to-body weight ratios did not differ from their WT littermates (Figure 7A through 7C). In addition, there were no significant differences in the echocardiographic, hemodynamic, and histological findings between the 2 groups, except that HCN2-Tg mice showed significantly faster heart rates than control WT mice (Figure 7D and 7E, and Table 2). Consistent with those results, there were no significant differences in the expression of the cardiac stress marker genes *ANP*, *BNP*, and *SERCA2* between the 2 groups (Figure 7F through 7H). Taken together, these findings demonstrate that increased ventricular expression of HCN2 and the resultant increase in the $I_f$ current by themselves are not sufficient to significantly alter cardiac structure or systolic function.

We also examined the effect of β-adrenergic stimulation on HCN2-Tg mice. When we used an osmotic mini pump to subcutaneously administer isoproterenol to HCN2-Tg and WT mice for a week, both genotypes showed comparable cardiac hypertrophic responses, as assessed from heart-to-body weight ratios (Figure 8A). Systolic function evaluated based on echocardiographic findings and blood pressure did not differ between the 2 genotypes treated with isoproterenol (Figure 8B and Table 3). Water intake was also not altered in either genotype treated with isoproterenol (Figure 8C). Heart rate in HCN2-Tg treated with isoproterenol was faster than those in WT mice treated with isoproterenol (Figure 8D), whereas the percentage increase induced by isoproterenol in heart rate was comparable between 2 genotypes (10.1% increase in WT mice versus 13.0% increase in HCN2-Tg mice). By contrast, continuous ECG monitoring during the administration of isoproterenol showed that PVC and VT frequencies were significantly higher in HCN2-Tg than WT mice (Figure 9A through 9C). Thus increased expression of ventricular HCN2 channels appears to promote susceptibility to isoproterenol-

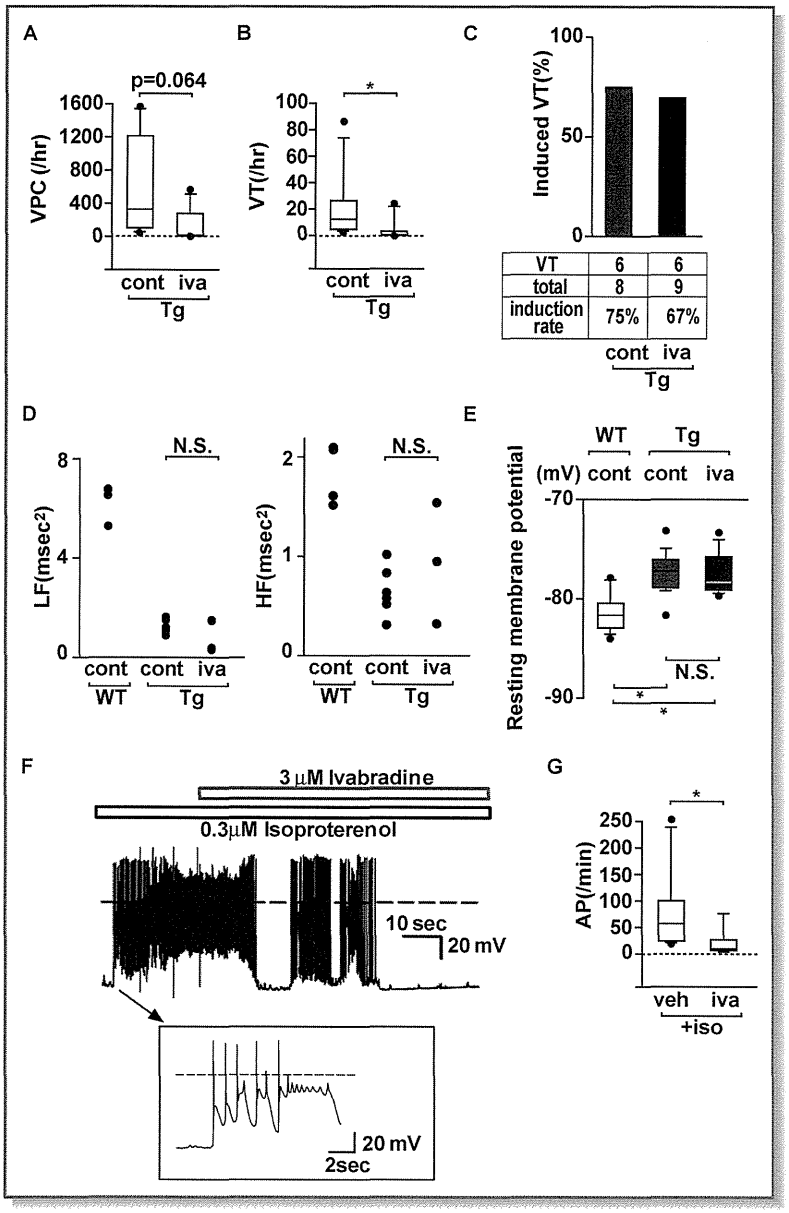


**Figure 5.** Ivabradine (iva) reduces arrhythmicity in dnNRSF-Tg (Tg) hearts. A and B, Numbers of PVCs (A) and VTs (B) recorded using a telemetry system in Tg mice treated with or without iva. Data are shown as box plots. Mann–Whitney test was used for analysis. *$P$<0.05 (n=7 for Tg without iva, 6 for Tg with iva). C, Frequency of mice with inducible VTs during intracardiac electrophysiology studies among Tg mice treated for 12 weeks with or without iva. VT, numbers of mice with inducible VT; total, total numbers of mice tested. D, Average power of the low frequency (LF) and high frequency (HF) components of HRVs recorded over a 24-hour period in untreated WT and Tg mice treated with or without iva. Mice treated without iva are indicated as cont. n=4 for WT without iva, n=6 for Tg without iva, n=4 for Tg with iva. Kruskal–Wallis nonparametric ANOVA followed by Bonferroni correction was used for the analysis. Data are shown as dot plots. E, Average resting membrane potentials recorded from ventricular myocytes isolated from 20-week-old untreated WT and Tg mice treated with or without iva: Kruskal–Wallis nonparametric ANOVA followed by the Bonferroni correction was used for the analysis. NS, not significant. *$P$<0.0166 vs WT (n=12 for untreated WT, 12 for untreated Tg, 14 for Tg with iva). Mice treated without iva are indicated as cont. Data are shown as box plots. F, Representative traces showing that ivabradine (3 μmol/L) reduces the frequency of spontaneous action potentials in the presence of isoproterenol (0.3 μmol/L) are shown. Arrows show larger pictures of action potentials. G, Graphs show numbers of spontaneous action potentials in the presence of isoproterenol (0.3 μmol/L) in ventricular myocytes from dnNRSF-Tg in the absence (veh) or presence of iva. Shown are the numbers of spontaneous action potentials (AP/min) occurring in the presence of isoproterenol (0.3 μmol/L) during the second minute after addition of iva or vehicle (veh). Data are shown as box plots. Mann–Whitney test was used for the analysis (n=6 for control and 5 for iva). *$P$<0.05. NS indicates not significant; dnNRSF-Tg indicates dominant-negative form of neuron-restrictive silencer factor transgenic mice; PVC, premature ventricular contraction; VT, ventricular tachycardia; ANOVA, analysis of variance; WT, wild type; cont, control; HRV, heart rate variability.

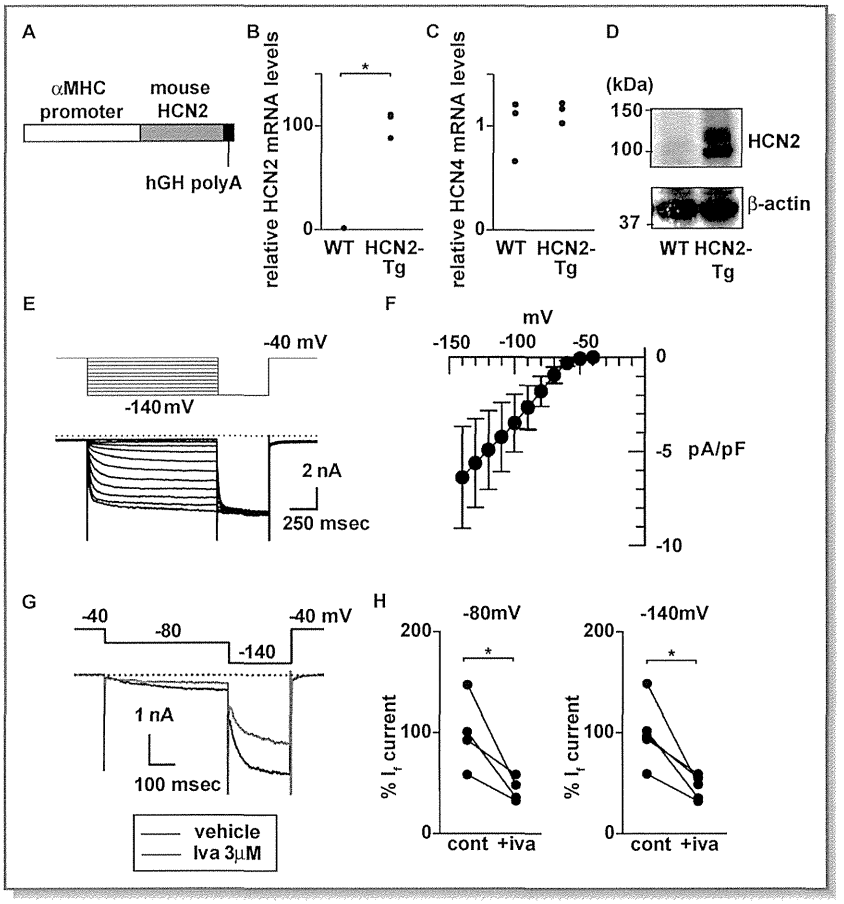


**Figure 6.** Generation of cardiac-specific HCN2 transgenic mice. A, Scheme of the construct for HCN2 transgenic mouse. hGH, human growth hormone. B and C, Relative levels of *HCN2* (B) and *HCN4* (C) mRNA in hearts from 12-week-old WT and HCN2-Tg mice. The Mann–Whitney test was used for the analysis. **P*<0.05 vs WT. n=3 in each group. Data are shown as dot plots. D, Representative Western blots for HCN2 and *β*-actin in ventricular myocytes from WT and HCN2-Tg mice. E, Representative $I_f$ currents recorded in ventricular myocytes from HCN2-Tg mice. Inward-rectifier $K^+$ current was suppressed by 0.5 mmol/L $BaCl_2$. F, Current-voltage relationship for $I_f$ in ventricular myocytes from HCN2-Tg mice. The amplitudes of time-dependent components activated by hyperpolarizing pulses were normalized by cellular capacitance (n=5). G, Effect of 3 μmol/L ivabradine (iva) (red line; 2 minutes after the application of iva) or vehicle (cont) on $I_f$ in ventricular myocytes from HCN2-Tg mice. H, Graphs show the suppressive effect of iva on $I_f$ amplitude at −80 mV (left panel, n=4 each) and −140 mV (right panel, n=5 each) in ventricular myocytes from HCN2-Tg mice. The mean relative $I_f$ amplitudes (%) in the absence of iva were assigned a value of 100. The Wilcoxon signed-rank test was used for the analysis. **P*<0.05 vs cont. HCN2-Tg indicates hyperpolarization-activated cyclic nucleotide-gated channel 2 transgenic mice; WT, wild type; cont, control; αMHC, α-myosin heavy chain.

induced cardiac arrhythmias without affecting cardiac structure or function.

When we then analyzed action potentials in ventricular myocytes isolated from HCN2-Tg and WT hearts, we found no apparent difference between the groups (Figure 9D). We then assessed the response of HCN2-Tg myocytes to *β*-adrenergic stimulation. After the application of 0.3 μmol/L isoproterenol, the resting membrane potential of ventricular myocytes isolated from HCN2-Tg hearts slowly depolarized, and started to fire spontaneously (Figure 9E), whereas such spontaneous activity was not induced in the myocytes from WT hearts. Ivabradine blocked the isoproterenol-related occurrence of spontaneous action potentials in ventricular myocytes from HCN2-Tg mice (Figure 9E and 9F). These data support our hypothesis that increased HCN channel expression in ventricular myocytes potentially increases the susceptibility to arrhythmias under sympathetic stimulation.

## Discussion

In healthy adult hearts, expression of HCN channels is restricted to the sinoatrial node and other parts of the conduction system. However, their expression is induced in the failing and hypertrophied ventricular myocardium.[6,7] In earlier studies, we showed that a transcriptional repressor, NRSF, negatively regulates the expression of the *HCN2* and *HCN4* genes and that a transcriptional activator, MEF2,

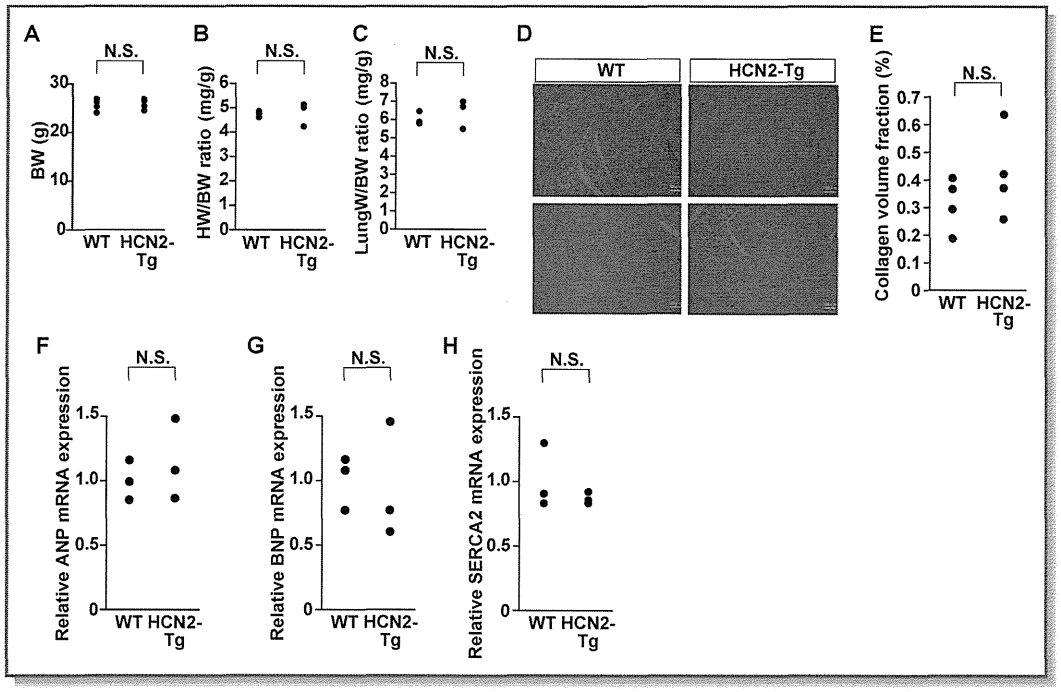


**Figure 7.** Features of cardiac-specific HCN2-Tg mice. A through C, Body weights (BW) (A), heart weight-to-body weight ratios (HW/BW) (B) and lung-to-body weight ratios (LW/BW) (C) in 12-week-old WT and HCN2-Tg mice are shown as dot plots (for BWs, n=4 for each group; for HW/BW ratios, n=3 for each group; and for LW/BW ratios, n=3 for each group). The Mann–Whitney test was used for the comparison between WT and HCN2-Tg. NS, not significant. D, Histology of WT and HCN2-Tg hearts from 12-week-old mice: Sirius-red staining. Magnification, ×400; scale bars, 100 μm. E, Graph showing the the percentage of collagen area in WT and HCN2-Tg mice (n=4 for each group). The Mann–Whitney test was used for the analysis. NS, not significant. Data are shown as dot plots. F through H, Relative levels of *ANP* (F), *BNP* (G), and *SERCA2* (H) mRNA in hearts from 12-week-old WT and HCN2-Tg mice (n=3 in each group). The Mann–Whitney test was used for the analysis. NS, not significant. Data are shown as dot plots in F through H. HCN2-Tg indicates hyperpolarization-activated cyclic nucleotide-gated channel 2 transgenic mice; WT, wild type.

**Table 2.** Hemodynamic Parameters in 8-Week-Old WT and HCN2-Tg Mice

| | WT | HCN2-Tg |
|---|---|---|
| Blood pressure, mm Hg | 103.3±2.9 | 104.8±2.3 |
| Heart rate, /min | 527±29.5 | 659±22.2* |
| Echocardiographic data | | |
| LVDd, mm | 2.53±0.12 | 2.53±0.08 |
| LVDs, mm | 1.15±0.10 | 1.08±0.07 |
| IVST, mm | 0.73±0.02 | 0.68±0.02 |
| PWT, mm | 0.72±0.03 | 0.73±0.02 |
| FS, % | 53.8±2.0 | 56.7±2.8 |

Values are means±SEM. Numbers of mice tested are 6 for each genotype. The Mann–Whitney test was used for comparison between WT and HCN2-Tg. WT indicates wild type; HCN2-Tg, hyperpolarization-activated cyclic nucleotide-gated channel 2 transgenic mice; LVDd, left ventricular diastolic dimension; LVDs, left ventricular systolic dimension; IVST, interventricular septum thickness; PWT, posterior wall thickness; FS, fractional shortening.

*$P$<0.05 vs control wild-type littermates.

positively regulates *HCN4* expression in cardiac myocytes.[9,25,26] Indeed, expression of both *HCN2* and *HCN4* is upregulated in dnNRSF-Tg mice, leading to an increase in the $I_f$ current in ventricular myocytes. Such increases in $I_f$ may predispose ventricular myocytes to enhanced automaticity, which can in turn trigger malignant arrhythmias. To clarify the contribution made by increased expression of HCN channels to the development of arrhythmias in dnNRSF-Tg mice, a useful model of heart failure with lethal arrhythmias, we tested the effects of ivabradine, a HCN channel blocker, on survival and arrhythmicity. We found that ivabradine significantly reduced the incidence of sudden death and malignant arrhythmias among dnNRSF-Tg mice without significantly reducing heart rate or affecting cardiac function, most likely by suppressing an increase in automaticity. We also confirmed the increased susceptibility to arrhythmias induced by β-adrenergic stimulation in mice specifically overexpressing the cardiac HCN2 channel. Collectively, our findings provide the first evidence that increased expression of HCN channels contributes to the increased arrhythmicity seen in failing hearts in vivo, and suggest that HCN channel blockade may represent a new and effective means of preventing sudden arrhythmic death in patients with heart failure.

There is now compelling evidence that $I_f$ currents play a key role in cardiac pacemaking.[27] Consistent with that idea,

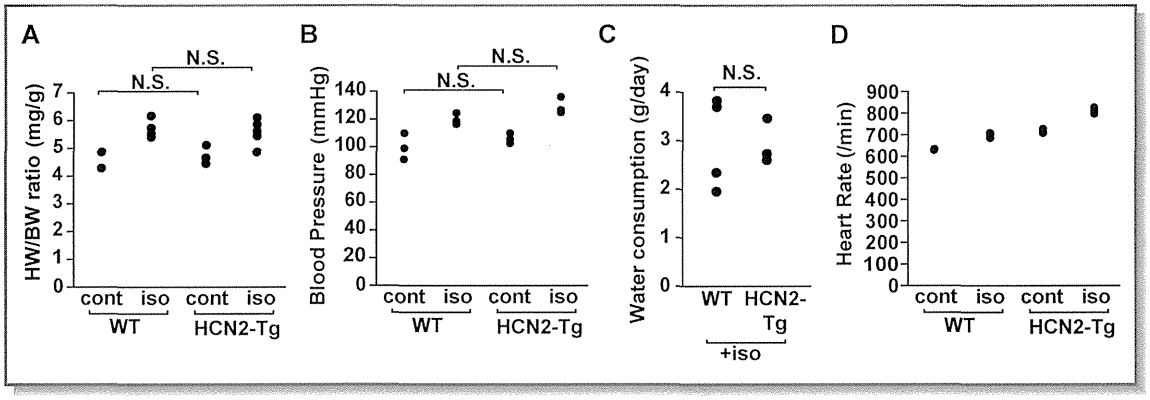


**Figure 8.** Effects of β-adrenergic stimulation in HCN2-Tg mice. A and B, HW/BW ratios (A) and blood pressures (B) in 24-week-old WT and HCN2-Tg mice, with or without 1 week of isoproterenol (iso) administration (15 mg/kg per day; subcutaneous infusion): *$P$<0.05. (for HW/BW ratios, n=3 for WT without iso, n=5 for WT with iso, n=3 for Tg without iso, n=5 for Tg with iso; for blood pressure, n=3 in each group). Mice treated without iso are indicated as cont. Kruskal–Wallis nonparametric ANOVA followed by the Bonferroni correction was used for analysis among the 4 groups. NS, not significant. All data are shown as dot plots. C, Water consumption (g/day) in 24-week-old WT and Tg mice treated for 1 week with iso (15 mg/kg per day; subcutaneous infusion) (n=4 for WT mice, n=3 for Tg mice). The Mann–Whitney test was used for the analysis. NS, not significant. Data are shown as dot plots. D, Heart rate assessed by ambulatory electrocardiography in 24-week-old WT and HCN2-Tg mice, with or without 1 week of isoproterenol (iso) administration (15 mg/kg per day; subcutaneous infusion): Kruskal–Wallis nonparametric ANOVA followed by the Bonferroni correction was used for analysis among the 4 groups. n=3 for each group. Data are shown as dot plots. HCN2-Tg indicates hyperpolarization-activated cyclic nucleotide-gated channel 2 transgenic mice; WT, wild type; cont, control; HW/BW, heart weight-to-body weight ratios; ANOVA, analysis of variance.

**Table 3.** Echocardiographic Data in 24-Week-Old WT and HCN2-Tg Mice Treated With Isoproterenol for 1 Week

| | WT+Iso | HCN2-Tg+Iso |
|---|---|---|
| LVDd, mm | 3.09±0.18 | 3.14±0.21 |
| LVDs, mm | 1.68±0.21 | 1.66±0.33 |
| FS, % | 46.4±4.1 | 49.6±7.8 |

Values are means±SEM. Numbers of mice tested are n=5 for WT treated with isoproterenol and 4 for HCN2-Tg treated with isoproterenol. The Mann–Whitney test was used for comparison between WT+Iso and HCN2-Tg+Iso.WT indicates wild type; HCN2-Tg, hyperpolarization-activated cyclic nucleotide-gated channel 2 transgenic mice; Iso, isoproterenol; LVDd, left ventricular diastolic dimension; LVDs, left ventricular systolic dimension; FS, fractional shortening.

an $I_f$ blocker, ivabradine, can reduce heart rate without exerting negative inotropic or vasodilatory effects.[28] As basal heart rate is an independent risk factor for mortality in patients with heart failure,[29,30] it had been thought that an agent that selectively lowered heart rate could improve outcomes in patients with heart failure. As would be expected, results from a recent clinical trial, the Systolic Heart failure treatment with the $I_f$ inhibitor ivabradine Trial (SHIFT), showed that among heart failure patients with resting heart rates of 70 beats/min or higher, the negative chronotropic effect of ivabradine significantly improved their outcomes.[31] In addition to this human clinical trial, several studies using animal models revealed the beneficial effects of ivabradine-induced heart rate reduction on cardiac structure and electrical remodeling.[32] In our present study, to evaluate the direct effects of ivabradine on the arrhythmicity of ventricular myocytes and the survival of dnNRSF-Tg mice, while avoiding the effects of heart rate reduction, we used a relatively low dose of ivabradine (7 mg/kg per day), which did not significantly affect heart rates in dnNRSF-Tg mice, though it did reduce heart rates by around 20% in WT mice (Table 1). This likely reflects the fact that basal heart rates were significantly lower in dnNRSF-Tg mice than WT mice (Table 1). From these findings, we conclude that the beneficial effects of ivabradine on arrhythmicity and survival in dnNRSF-Tg mice largely reflect direct suppression of arrhythmicity in ventricular myocytes, independent of heart rate, although the possibility that ivabradine prevents deaths due to congestive heart failure in some dnNRSF-Tg mice cannot be excluded completely. The observation that HCN channels and $I_f$ currents are upregulated in the ventricular myocardium of hypertrophied and failing hearts in both rodent models and humans[6,7] suggests that, in some clinical settings, ivabradine may improve the outcomes of patients with heart failure by both reducing heart rate and acting via mechanisms independent of heart rate reduction.

Our results showing that ivabradine did not prevent cardiac dysfunction and structural remodeling in dnNSRF-Tg mice under conditions in which heart rate was not significantly reduced by the drug, suggest that increased $I_f$ amplitude in ventricular myocytes does not contribute substantially to cardiac structural remodeling and depressed systolic function.

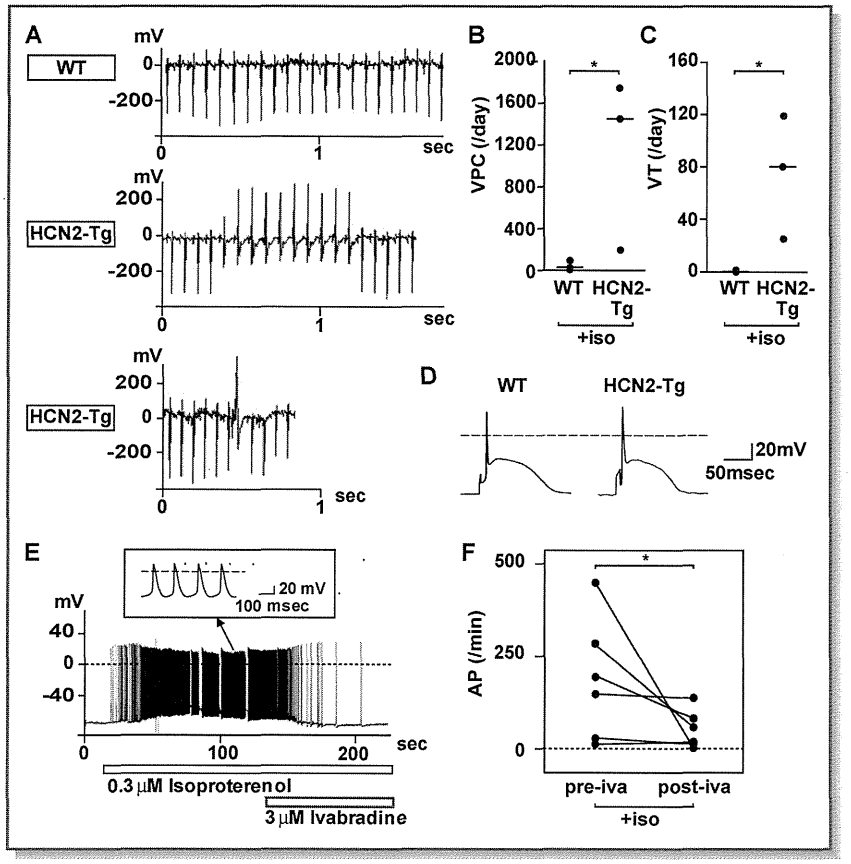


**Figure 9.** *β*-adrenergic stimulation-induced ventricular arrhythmias in HCN2-Tg hearts. A, Representative ECG traces showing sinus rhythm in WT mice treated with isoproterenol (upper panel) and ventricular tachycardia (VT) with atrioventricular dissociation (middle panel) and isolated PVC (lower panel) in HCN2-Tg mice treated with isoproterenol. B and C, Numbers of isolated PVCs (B) and VTs (C) recorded using a telemetry system in WT and HCN2-Tg mice treated with isoproterenol (iso). Mann–Whitney test was used for the analysis. **P*<0.05 (n=3 for each group). D, Representative traces of action potentials recorded in ventricular myocytes isolated from WT and HCN2-Tg hearts. E, Representative traces of spontaneous action potentials in ventricular myocytes from HCN2-Tg hearts recorded in the presence of 0.3 μmol/L isoproterenol, to which 3 μmol/L ivabradine was subsequently added, as indicated. Arrows show larger pictures of action potentials. F, Graph showing the numbers of spontaneous action potentials (AP) in the presence of 0.3 μmol/L isoproterenol (iso) in ventricular myocytes from HCN2-Tg mice with or without 3 μmol/L ivabradine (iva). The Wilcoxon signed-rank test was used for the analysis. Shown are the numbers of action potentials occurring during the minute just before (pre-iva) and the second minute after (post-iva) addition of ivabradine. **P*<0.05 (n=6). HCN2-Tg indicates hyperpolarization-activated cyclic nucleotide-gated channel 2 transgenic mice; WT, wild type; PVC, premature ventricular contraction.

Our finding that cardiac-specific overexpression of *HCN2* and the corresponding increase in $I_f$ amplitude did not affect cardiac structure or systolic function support this notion. These results suggest the beneficial effects of ivabradine on cardiac structural remodeling and dysfunction observed in several animal models and in human patients with heart failure largely depend on its effect on heart rate mediated through suppression of $I_f$ currents in the sinus node.[31,32] This is consistent with a recent subanalysis of the morBidity-mortality EvAlUaTion of the $I_f$ inhibitor ivabradine in patients with CAD and left ventricULar dysfunction (BEAUTIFUL) study, in which the impact of ivabradine treatment on cardiovascular outcome in patients with stable coronary artery disease and left ventricular systolic dysfunction was tested. Echocardiography revealed that the reduction in the left ventricular systolic volume index seen with ivabradine treatment was related to the degree of heart rate reduction.[33,34] In addition, a subanalysis of the SHIFT study, in which the effects of ivabradine treatment on outcome in heart failure patients with resting heart rates >70 beats/min were studied, also showed that the improvement in left ventricular systolic function seen with ivabradine treatment was associated with a decrease in heart rate.[31,35]

Sudden cardiac death is generally caused by ventricular tachycardia or fibrillation. These arrhythmias occur due to the simultaneous presence of abnormal impulse initiation (the trigger), which results from either enhanced automaticity or triggered activity, and a preexisting arrhythmogenic

substrates for the initiation and maintenance of reentry.[36,37] In dnNRSF-Tg mice, in vivo electrophysiological analysis showed that ivabradine failed to attenuate the increase in susceptibility to induced arrhythmias dependent on the presence of arrhythmogenic substrates. Ivabradine did not prevent the generation of arrhythmogenic substrates in dnNRSF-Tg hearts, which is consistent with the results showing that ivabradine does not affect cardiac structural remodeling, including the fibrosis and cardiac dysfunction seen in dnNRSF-Tg mice. This suggests that increased ventricular expression of HCN channels contributes to the generation of arrhythmogenic triggers but not to the generation of arrhythmogenic substrates. The fact that cardiac-specific overexpression of HCN2 did not alter the normal cardiac structure and systolic function supports this finding. These observations are also consistent with recent reports showing that mice lacking both cardiac HCN2 and HCN4 developed cardiac hypertrophy in response to pressure overload induced by transaortic constriction (TAC), like WT mice do, whereas ventricular myocytes isolated from the double knockout mice subjected to TAC showed weaker proarrhythmogenic parameters than those from WT mice subjected to TAC.[38] The potential contribution made by ventricular HCN channels to the repolarization process was also apparent in ventricular myocytes from knockout mice lacking HCN3 or HCN1,[39] which can contribute to an increase in arrhythmogenic triggers. Still, it is possible that ivabradine also inhibits the generation of arrhythmogenic substrates, such as interstitial fibrosis, thereby suppressing the susceptibility to induced arrhythmias under conditions where it reduces heart rates, as stated above. Further studies in other animal models of cardiac disease and in humans with heart failure would be of great interest.

The autonomic control of heart rate and sinoatrial node activity is largely mediated by the $I_f$ current, which is specifically modulated by intracellular cAMP.[40] Thus, upregulation of HCN channels may enhance the arrhythmicity of failing ventricular myocytes exposed to $\beta$-adrenergic stimulation. Consistent with this notion, ventricular myocytes from dnNRSF-Tg mice showed abnormal spontaneous action potentials when exposed to isoproterenol,[14] and this effect was attenuated by ivabradine (Figure 5F and 5G). Similarly, ventricular myocytes from HCN2-Tg mice exhibited spontaneous action potentials in the presence of isoproterenol, and that effect too was inhibited by ivabradine (Figure 9E and 9F). By contrast, this response was not seen in myocytes from WT hearts. These results suggest that upregulation of HCN channels, and the resultant increase in $I_f$ currents predispose failing hearts to arrhythmias in a setting of enhanced sympathetic drive. Indeed, in an earlier study, we showed that activation of sympathetic activity contributes to sudden death in dnNRSF-Tg mice;[14] moreover, our present findings show that HCN2-Tg mice are highly susceptible to isoproterenol-induced arrhythmias.

Ivabradine was developed for clinical use in the treatment of stable angina pectoris as a heart rate-lowering agent and was recently shown to significantly improve outcomes in patients with heart failure and elevated heart rate (70 beats/min or above).[28,31,40] Although in the SHIFT study sudden cardiac death did not appear to be affected by ivabradine,[31] this finding may be attributed to the effect of background treatment with a $\beta$-blocker (used in 89% of patients), which effectively prevents sudden cardiac death.[41,42] A recently published post hoc subgroup analysis of SHIFT study showed that reduction of cardiovascular death by ivabradine among subjects without $\beta$-blocker treatment was not statistically significant.[43] However, the numbers of subjects without $\beta$-blocker treatment is much smaller than the overall sample size to detect effects of ivabradine. Further investigation will be needed to determine whether ivabradine will prevent sudden cardiac death in heart failure patients who cannot tolerate a $\beta$-blocker.

## Acknowledgments

We thank Ms Yukari Kubo for her excellent secretarial work and Ms Aoi Fujishima and Ms Akiko Abe for their excellent technical support.

## Sources of Funding

This research was supported by Grants-in-Aid for Scientific Research from the Japan Society for the Promotion of Science (to Drs Kuwahara, Kinoshita, Takano, Nakagawa, and Nakao), and a grant from the Japanese Ministry of Health, Labor, and Welfare (to Dr Nakao), and by grants from Institut de Recherches Internationales Servier, the Japan Foundation for Applied Enzymology, the UBE foundation, the Ichiro Kanehara Foundation, the Takeda Science Foundation, the Hoh-ansha Foundation, and the SENSHIN Medical Research Foundation (to Dr Kuwahara).

## Disclosure

This work was supported, in part, by a grant from Institut de Recherches Internationales Servier (to Dr Kuwahara).

## References

1. Tomaselli GF, Marban E. Electrophysiological remodeling in hypertrophy and heart failure. *Cardiovasc Res*. 1999;42:270–283.
2. Robinson RB, Siegelbaum SA. Hyperpolarization-activated cation currents: from molecules to physiological function. *Annu Rev Physiol*. 2003;65:453–480.
3. Wahl-Schott C, Biel M. HCN channels: structure, cellular regulation and physiological function. *Cell Mol Life Sci*. 2009;66:470–494.
4. Yasui K, Liu W, Opthof T, Kada K, Lee JK, Kamiya K, Kodama I. I(f) current and spontaneous activity in mouse embryonic ventricular myocytes. *Circ Res*. 2001;88:536–542.

5. Cerbai E, Pino R, Sartiani L, Mugelli A. Influence of postnatal-development on I (f) occurrence and properties in neonatal rat ventricular myocytes. *Cardiovasc Res*. 1999;42:416–423.
6. Cerbai E, Mugelli A. I(f) in non-pacemaker cells: role and pharmacological implications. *Pharmacol Res*. 2006;53:416–423.
7. Stillitano F, Lonardo G, Zicha S, Varro A, Cerbai E, Mugelli A, Nattel S. Molecular basis of funny current (If) in normal and failing human heart. *J Mol Cell Cardiol*. 2008;45:289–299.
8. Kuwahara K, Saito Y, Ogawa E, Takahashi N, Nakagawa Y, Naruse Y, Harada M, Hamanaka I, Izumi T, Miyamoto Y, Kishimoto I, Kawakami R, Nakanishi M, Mori N, Nakao K. The neuron-restrictive silencer element-neuron-restrictive silencer factor system regulates basal and endothelin 1-inducible atrial natriuretic peptide gene expression in ventricular myocytes. *Mol Cell Biol*. 2001; 21:2085–2097.
9. Kuwahara K, Saito Y, Takano M, Arai Y, Yasuno S, Nakagawa Y, Takahashi N, Adachi Y, Takemura G, Horie M, Miyamoto Y, Morisaki T, Kuratomi S, Noma A, Fujiwara H, Yoshimasa Y, Kinoshita H, Kawakami R, Kishimoto I, Nakanishi M, Usami S, Saito Y, Harada M, Nakao K. NRSF regulates the fetal cardiac gene program and maintains normal cardiac structure and function. *EMBO J*. 2003; 22:6310–6321.
10. Xia S, Wang Y, Zhang Y, Deng SB, Du JL, Wang XC, She Q. Dynamic changes in HCN2, HCN4, KCNE1, and KCNE2 expression in ventricular cells from acute myocardial infarction rat hearts. *Biochem Biophys Res Commun*. 2010; 395:330–335.
11. Fernandez-Velasco M, Ruiz-Hurtado G, Delgado C. I K1 and I f in ventricular myocytes isolated from control and hypertrophied rat hearts. *Pflugers Arch*. 2006;452:146–154.
12. Du XJ, Feng X, Gao XM, Tan TP, Kiriazis H, Dart AM. I(f) channel inhibitor ivabradine lowers heart rate in mice with enhanced sympathoadrenergic activities. *Br J Pharmacol*. 2004;142:107–112.
13. Leoni AL, Marionneau C, Demolombe S, Le Bouter S, Mangoni ME, Escande D, Charpentier F. Chronic heart rate reduction remodels ion channel transcripts in the mouse sinoatrial node but not in the ventricle. *Physiol Genomics*. 2005;24:4–12.
14. Kinoshita H, Kuwahara K, Takano M, Arai Y, Kuwabara Y, Yasuno S, Nakagawa Y, Nakanishi M, Harada M, Fujiwara M, Murakami M, Ueshima K, Nakao K. T-type $Ca^{2+}$ channel blockade prevents sudden death in mice with heart failure. *Circulation*. 2009;120:743–752.
15. Bucchi A, Tognati A, Milanesi R, Baruscotti M, DiFrancesco D. Properties of ivabradine-induced block of HCN1 and HCN4 pacemaker channels. *J Physiol*. 2006;572:335–346.
16. Gehrmann J, Berul CI. Cardiac electrophysiology in genetically engineered mice. *J Cardiovasc Electrophysiol*. 2000;11:354–368.
17. Kawakami R, Saito Y, Kishimoto I, Harada M, Kuwahara K, Takahashi N, Nakagawa Y, Nakanishi M, Tanimoto K, Usami S, Yasuno S, Kinoshita H, Chusho H, Tamura N, Ogawa Y, Nakao K. Overexpression of brain natriuretic peptide facilitates neutrophil infiltration and cardiac matrix metalloproteinase-9 expression after acute myocardial infarction. *Circulation*. 2004;110:3306–3312.
18. Just A, Faulhaber J, Ehmke H. Autonomic cardiovascular control in conscious mice. *Am J Physiol Regul Integr Comp Physiol*. 2000;279:R2214–R2221.
19. Stieber J, Wieland K, Stockl G, Ludwig A, Hofmann F. Bradycardic and proarrhythmic properties of sinus node inhibitors. *Mol Pharmacol*. 2006;69: 1328–1337.
20. Mukoyama M, Nakao K, Hosoda K, Suga S, Saito Y, Ogawa Y, Shirakami G, Jougasaki M, Obata K, Yasue H, Kambayashi Y, Inouye K, Imura H. Brain natriuretic peptide as a novel cardiac hormone in humans. Evidence for an exquisite dual natriuretic peptide system, atrial natriuretic peptide and brain natriuretic peptide. *J Clin Invest*. 1991;87:1402–1412.
21. Nakagawa O, Ogawa Y, Itoh H, Suga S, Komatsu Y, Kishimoto I, Nishino K, Yoshimasa T, Nakao K. Rapid transcriptional activation and early mrna turnover of brain natriuretic peptide in cardiocyte hypertrophy. Evidence for brain natriuretic peptide as an "emergency" cardiac hormone against ventricular overload. *J Clin Invest*. 1995;96:1280–1287.
22. La Rovere MT, Pinna GD, Maestri R, Mortara A, Capomolla S, Febo O, Ferrari R, Franchini M, Gnemmi M, Opasich C, Riccardi PG, Traversi E, Cobelli F. Short-term heart rate variability strongly predicts sudden cardiac death in chronic heart failure patients. *Circulation*. 2003;107:565–570.
23. Sandercock GR, Brodie DA. The role of heart rate variability in prognosis for different modes of death in chronic heart failure. *Pacing Clin Electrophysiol*. 2006;29:892–904.
24. Takano M, Kinoshita H, Shioya T, Itoh M, Nakao K, Kuwahara K. Pathophysiological remodeling of mouse cardiac myocytes expressing dominant negative mutant of neuron restrictive silencing factor. *Circ J*. 2010;74:2712–2719.
25. Kuratomi S, Ohmori Y, Ito M, Shimazaki K, Muramatsu S, Mizukami H, Uosaki H, Yamashita JK, Arai Y, Kuwahara K, Takano M. The cardiac pacemaker-specific channel HCN4 is a direct transcriptional target of MEF2. *Cardiovasc Res*. 2009;83:682–687.
26. Kuratomi S, Kuratomi A, Kuwahara K, Ishii TM, Nakao K, Saito Y, Takano M. NRSF regulates the developmental and hypertrophic changes of HCN4 transcription in rat cardiac myocytes. *Biochem Biophys Res Commun*. 2007; 353:67–73.
27. Baruscotti M, Bucchi A, Viscomi C, Mandelli G, Consalez G, Gnecchi-Rusconi T, Montano N, Casali KR, Micheloni S, Barbuti A, DiFrancesco D. Deep bradycardia and heart block caused by inducible cardiac-specific knockout of the pacemaker channel gene HCN4. *Proc Natl Acad Sci USA*. 2011; 108:1705–1710.
28. Riccioni G. Ivabradine: recent and potential applications in clinical practice. *Expert Opin Pharmacother*. 2011;12:443–450.
29. Bohm M, Swedberg K, Komajda M, Borer JS, Ford I, Dubost-Brama A, Lerebours G, Tavazzi L. Heart rate as a risk factor in chronic heart failure (SHIFT): the association between heart rate and outcomes in a randomised placebo-controlled trial. *Lancet*. 2010;376:886–894.
30. Fox K, Borer JS, Camm AJ, Danchin N, Ferrari R, Lopez Sendon JL, Steg PG, Tardif JC, Tavazzi L, Tendera M. Resting heart rate in cardiovascular disease. *J Am Coll Cardiol*. 2007;50:823–830.
31. Swedberg K, Komajda M, Bohm M, Borer JS, Ford I, Dubost-Brama A, Lerebours G, Tavazzi L. Ivabradine and outcomes in chronic heart failure (SHIFT): a randomised placebo-controlled study. *Lancet*. 2010;376: 875–885.
32. Heusch G, Skyschally A, Schulz R. Cardioprotection by ivabradine through heart rate reduction and beyond. *J Cardiovasc Pharmacol Ther*. 2011;16:281–284.
33. Ceconi C, Freedman SB, Tardif JC, Hildebrandt P, McDonagh T, Gueret P, Parrinello G, Robertson M, Steg PG, Tendera M, Ford I, Fox K, Ferrari R. Effect of heart rate reduction by ivabradine on left ventricular remodeling in the echocardiographic substudy of beautiful. *Int J Cardiol*. 2011;146:408–414.
34. Fox K, Ford I, Steg PG, Tendera M, Ferrari R. Ivabradine for patients with stable coronary artery disease and left-ventricular systolic dysfunction (BEAUTIFUL): a randomised, double-blind, placebo-controlled trial. *Lancet*. 2008;372:807–816.
35. Tardif JC, O'Meara E, Komajda M, Bohm M, Borer JS, Ford I, Tavazzi L, Swedberg K. Effects of selective heart rate reduction with ivabradine on left ventricular remodelling and function: results from the shift echocardiography substudy. *Eur Heart J*. 2011;32:2507–2515.
36. Boukens BJ, Christoffels VM, Coronel R, Moorman AF. Developmental basis for electrophysiological heterogeneity in the ventricular and outflow tract myocardium as a substrate for life-threatening ventricular arrhythmias. *Circ Res*. 2009;104:19–31.
37. Sasyniuk BI. Symposium on the management of ventricular dysrhythmias. Concept of reentry versus automaticity. *Am J Cardiol*. 1984;54:1A–6A.
38. Hofmann F, Fabritz L, Stieber J, Schmitt J, Kirchhof P, Ludwig A, Herrmann S. Ventricular HCN channels decrease the repolarization reserve in the hypertrophic heart. *Cardiovasc Res*. 2012;95:317–326.
39. Fenske S, Krause S, Biel M, Wahl-Schott C. The role of HCN channels in ventricular repolarization. *Trends Cardiovasc Med*. 2011;21:216–220.
40. DiFrancesco D. The role of the funny current in pacemaker activity. *Circ Res*. 2010;106:434–446.
41. Effect of metoprolol CR/XL in chronic heart failure: metoprolol CR/XL randomised intervention trial in congestive heart failure (MERIT-HF). *Lancet*. 1999;353:2001–2007.
42. Packer M, Fowler MB, Roecker EB, Coats AJ, Katus HA, Krum H, Mohacsi P, Rouleau JL, Tendera M, Staiger C, Holcslaw TL, Amann-Zalan I, DeMets DL. Effect of carvedilol on the morbidity of patients with severe chronic heart failure: results of the carvedilol prospective randomized cumulative survival (COPERNICUS) study. *Circulation*. 2002;106:2194–2199.
43. Swedberg K, Komajda M, Bohm M, Borer J, Robertson M, Tavazzi L, Ford I. Effects on outcomes of heart rate reduction by ivabradine in patients with congestive heart failure: is there an influence of beta-blocker dose? Findings from the SHIFT (systolic heart failure treatment with the I(f) inhibitor ivabradine trial) study. *J Am Coll Cardiol*. 2012;59: 1938–1945.

Cardiovascular Research (2013) **99**, 657–664
doi:10.1093/cvr/cvt128

# Cardiac nuclear high mobility group box 1 prevents the development of cardiac hypertrophy and heart failure

**Akira Funayama[1], Tetsuro Shishido[1]*, Shunsuke Netsu[1], Taro Narumi[1], Shinpei Kadowaki[1], Hiroki Takahashi[1], Takuya Miyamoto[1], Tetsu Watanabe[1], Chang-Hoon Woo[2], Jun-ichi Abe[3], Koichiro Kuwahara[4], Kazuwa Nakao[4], Yasuchika Takeishi[5], and Isao Kubota[1]**

[1]Department of Cardiology, Pulmonology, and Nephrology, Yamagata University School of Medicine, 2-2-2 Iida-Nishi, Yamagata 990-9585, Japan; [2]Department of Pharmacology, College of Medicine, Yeungnam University, Daegu, Korea; [3]Aab Cardiovascular Research Institute, University of Rochester, Rochester, NY, USA; [4]Department of Medicine and Clinical Science, Kyoto University Graduate School of Medicine, Kyoto, Japan; and [5]Department of Cardiology and Hematology, Fukushima Medical University, Fukushima, Japan

*Received 5 September 2012; revised 25 March 2013; accepted 18 May 2013; online publish-ahead-of-print 25 May 2013*

**Time for primary review: 32 days**

**Aims** High mobility group box 1 (HMGB1) is an abundant and ubiquitous nuclear DNA-binding protein that has multiple functions dependent on its cellular location. HMGB1 binds to DNA, facilitating numerous nuclear functions including maintenance of genome stability, transcription, and repair. However, little is known about the effects of nuclear HMGB1 on cardiac hypertrophy and heart failure. The aim of this study was to examine whether nuclear HMGB1 plays a role in the development of cardiac hypertrophy induced by pressure overload.

**Methods and results** Analysis of human biopsy samples by immunohistochemistry showed decreased nuclear HMGB1 expression in failing hearts compared with normal hearts. Nuclear HMGB1 decreased in response to both endothelin-1 (ET-1) and angiotensin II (Ang II) stimulation in neonatal rat cardiomyocytes, where nuclear HMGB1 was acetylated and translocated to the cytoplasm. Overexpression of nuclear HMGB1 attenuated ET-1 induced cardiomyocyte hypertrophy. Thoracic transverse aortic constriction (TAC) was performed in transgenic mice with cardiac-specific overexpression of HMGB1 (HMGB1-Tg) and wild-type (WT) mice. Cardiac hypertrophy after TAC was attenuated in HMGB1-Tg mice and the survival rate after TAC was higher in HMGB1-Tg mice than in WT mice. Induction of foetal cardiac genes was decreased in HMGB1-Tg mice compared with WT mice. Nuclear HMGB1 expression was preserved in HMGB1-Tg mice compared with WT mice and significantly attenuated DNA damage after TAC was attenuated in HMGB1-TG mice.

**Conclusion** These results suggest that the maintenance of stable nuclear HMGB1 levels prevents hypertrophy and heart failure by inhibiting DNA damage.

**Keywords** HMGB1 • Heart failure • Acetylation • Translocation • Pressure overload

## 1. Introduction

Cardiac hypertrophy is associated with many forms of heart disease, including ischaemic disease, hypertensive heart disease, and valvular stenosis, and is a major risk factor for the development of heart failure and death.[1,2] Despite advances in the treatment of heart failure, it is still one of the leading causes of death in industrialized countries.[3] Therefore, elucidation of the mechanisms underlying the progression of cardiac hypertrophy to heart failure is important to develop effective therapeutic strategies for the treatment of heart failure.[4]

High mobility group box 1 (HMGB1) is a nuclear DNA-binding protein present in various types of cells, which functions in maintaining nucleosome structure, and regulating gene transcription, replication, and DNA repair.[5,6] The high degree of conservation among species and organs implies that HMGB1 plays a critical role in the modulation of cellular functions. HMGB1 knockout mice die shortly after birth

* Corresponding author. Tel: +81 23 628 5302; Fax: +81 23 628 5305, Email: tshishid@med.id.yamagata-u.ac.jp

and show severe hypoglycaemia, indicating that HMGB1 is essential for survival.[7] Recent reports investigating the functions of HMGB1 have mainly focused on the extracellular regulation of cells by HMGB1,[8] because in addition to its nuclear activity, HMGB1 functions as a cytokine.[9] In inflammatory diseases such as sepsis, HMGB1 is translocated from the nucleus to the cytoplasm and is actively secreted into the extracellular environment, where it interacts with several surface molecules, including the receptor for advanced glycation end-products and Toll-like receptors.[9,10] Extracellular HMGB1 also regulates both inflammation and regenerating processes.[11] In the presence of tissue damage, HMGB1 released from inflammatory cells and necrotic cells stimulates monocytes/macrophages to secrete inflammatory cytokines amplifying the inflammatory response. We have shown that coronary artery ligation in transgenic mice with cardiac-specific overexpression of HMGB1 (HMGB1-TG) resulted in enhanced angiogenesis, improved survival, and restored cardiac function compared with wild-type (WT) mice.[12] In contrast, Andrassy *et al.*[13] have shown that serum levels of HMGB-1 are associated with infarct size and the degree of cardiac remodelling in patients with myocardial infarction.

It has been reported in recent years that DNA damage is involved in the progression of heart failure.[14] HMGB1 was discovered as a chromatin-binding protein, and is known to adjust transcription and indirectly adjust DNA damage.[15] Previous studies have shown that post-translational modification by acetylation of lysine residues is crucial for the translocation of HMGB1 in hepatocytes and immune cells.[16,17] Because nuclear HMGB1 plays a critical role in the regulation of DNA repair systems,[15] mitochondrial functions,[18] gene-specific DNA-binding,[19] and morphology in aging and neurodegenerative disorders,[20,21] it is suspected that translocation of HMGB1 from the nucleus might modify cellular function. However, the role of nuclear HMGB1 in cardiac hypertrophy and heart failure is not known. In the present study, we examined the role of nuclear HMGB1 in protecting the heart during pressure overload.

# 2. Methods

The methods/protocols used in the present study are detailed in the Supplementary material online.

## 2.1 Materials and reagents

Endothelin-1 (ET-1) and angiotensin II (Ang II) were purchased from Sigma-Aldrich Japan (Tokyo, Japan). The antibody against HMGB1 was obtained from Shino-Test Corporation (Sagamihara, Japan). Antibodies against acetyl-lysine and β-tubulin were obtained from Cell Signaling Technology (Danvers, MA, USA). The anti-8-hydroxy-2′-desoxiguanosine (8-OHdG) antibody was obtained from Nikken Seil (Tokyo, Japan), and the anti-histone H3 antibody was obtained from MAB Institute, Inc. (Sapporo, Japan). The anti-actinin was obtained from Sigma-Aldrich Japan (Tokyo, Japan). The anti-platelet endothelial cell adhesion molecule was obtained from Cedarlane Laboratories Limited (Ontario, Canada). Primers for quantitative real-time reverse transcriptase–PCR were designed on the basis of GenBank sequences [mouse atrial natriuretic peptide (ANP), K02781; mouse brain natriuretic peptide (BNP), NM 008726; rat ANP, NM 012612.2; β- myosin heavy chain (β-MHC), AY 056464 and GAPDH, NM001001303]. Luciferase reporter constructs (hANP/luc and BNP/luc) were generated, and were used to examined the effect of nuclear HMGB1 on foetal gene expression.[22,23] The pGEX-5X-1 plasmids were kindly provided by Ikuo Maruyama (Kagoshima University Faculty of Medicine, Kagoshima, Japan).

## 2.2 Assessment of HMGB1 localization in human heart samples

Samples of the ventricle of three patients with heart failure and three control patients who were assessed to rule out cardiomyopathy and had normal cardiac function were used in the study (*Table 1*). Written informed consent was obtained from all the patients before the study. The protocol was performed in accordance to the Helsinki Declaration and was approved by the human investigations committee of our institution. Biopsy samples were immediately washed in phosphate buffered saline (PBS) before being snap-frozen in liquid nitrogen for immunofluorescent co-staining and biomechanical measurements. Fresh frozen 20 μm tissue sections were treated with a blocking agent prior to the addition of primary antibody at a dilution of 1:100. Sections were then treated with goat anti-rabbit Alexa Fluor 568 (Invitrogen, Carlsbad, CA, USA) at a dilution of 1:200. Samples were counterstained with Phalloidin (Invitrogen) and 4′,6-diamidino-2-phenylindole (DAPI) (Lonza, Walkersville, MD, USA). For analysis, nuclear positive cells were counted (five random fields to yield ~300 cardiomyocyte nuclei/section) and expressed as the percentage of the total number of cardiomyocytes.

## 2.3 Cultured neonatal rat cardiomyocytes

Hearts were collected from 1- to 2-day-old neonatal rat pups, promptly after euthanasia by decapitation, and primary cultures of neonatal rat cardiomyocytes were performed as described previously.[24,25] After serum starvation, neonatal rat cardiomyocytes were stimulated with ET-1 or Ang II, and samples were collected to examine the expression levels of HMGB1 by western blot analysis and ANP mRNA by quantitative RT–PCR. HMGB1 siRNA was purchased from Thermo Scientific Dharmacon (Lafayette, CO, USA) and used to transfect cardiomyocytes by using GenomOne-Neo (Ishihara Sangyo Kaisha, Osaka, Japan) according to the manufacturer's instructions. ET-1 inducible ANP and BNP promoter activities were evaluated by

**Table 1 Characteristics of patients with heart failure and healthy controls**

| Age (years) | Gender | Status | Aetiology of heart failure | BNP (pg/mL) | LVEF (%) | LVDd (mm) |
|---|---|---|---|---|---|---|
| 62 | Male | Normal | — | 40 | 74 | 43 |
| 55 | Male | Normal | — | 8 | 77 | 53 |
| 19 | Male | Normal | — | 31 | 79 | 50 |
| 82 | Female | Heart failure | dHCM | 376 | 36 | 48 |
| 71 | Male | Heart failure | HHD | 334 | 29 | 62 |
| 78 | Female | Heart failure | dHCM | 270 | 44 | 55 |

BNP, brain natriuretic peptide; LVEF, left-ventricular ejection fraction; LVDd, left-ventricular end-diastolic dimension; LVMI, LV mass index; dHCM, dilated phase of hypertrophic cardiomyopathy; HHD, hypertensive heart disease.

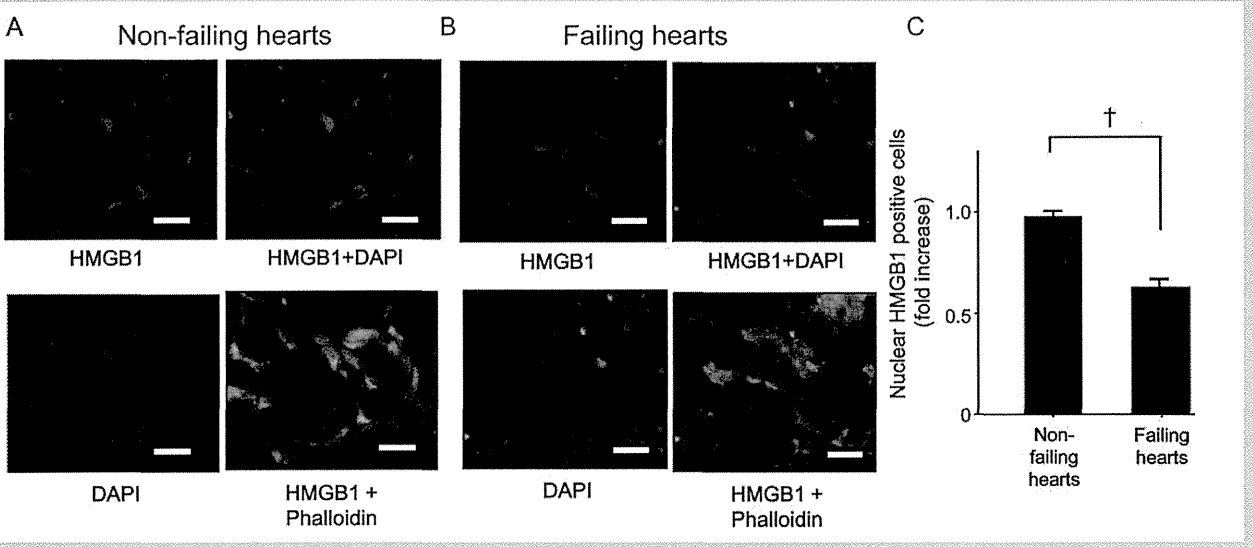


**Figure 1** Decreased nuclear HMGB1 in the failing heart. (*A*) Non-failing (left) and failing (right) human heart tissues were labelled with antibodies against HMGB1 (red) and phalloidin (green). Nuclei were stained with DAPI (blue). Bars, 50 μm. (*B*) Quantification of nuclear HMGB1 immunofluorescence data. Bars represent means ± SEM.

luciferase reporter gene assay with hANP/luc and BNP/luc, and the pRL-TK vector (Promega, Madison, WI, USA).[26,27] Expression vector transfection was performed using Lipofectamine LTX plus (Invitrogen) according to the manufacturer's instructions. Transcriptional activities were calculated from three separate assays performed in triplicate. Cardiomyocytes transfected with pmax-GFP (Lonza) and an HMGB1 expression vector or control vector for 24 h were incubated with or without ET-1 (100 nM) for an additional 48 h for cell surface area measurements using Image J software (US National Institutes of Health, Bethesda, MD, USA).

## 2.4 Pressure overload models

Eight to 10-week-old transgenic mice with cardiac-specific overexpression of HMGB1 (HMGB1-Tg)[12] and WT littermates were anaesthetized by intraperitoneal injection with a mixture of ketamine (80 mg/kg/h) and xylazine (8 mg/kg/h), intubated, and artificially ventilated as previously described. Pressure overload was then produced by thoracic transverse aortic constriction (TAC). Standard lead II ECG was recorded throughout the experiment, and the adequacy of anaesthesia was monitored from the disappearance of pedal withdrawal reflex. Cardiac function at 4 weeks after TAC or sham operation was evaluated by transthoracic echocardiography using an FFsonic 8900 (Fukuda Denshi Co., Tokyo, Japan) equipped with a 13 MHz phased-array transducer under anaesthesia with an intraperitoneal administration of pentobarbital sodium (35 mg/kg). Adequacy of anaesthesia was monitored at all times by assessment of skeletal muscle tone, respiration rate and rhythm, and response to tail pinch. Left-ventricular fractional shortening (LVFS) was calculated as [(LVEDD − LVESD)/LVEDD] × 100 (%). These mice and sham-operated ones were sacrificed by intraperitoneal injection of ketamine (1 g/kg) and xylazine (100 mg/kg), and hearts were rapidly excised. Mouse ANP and BNP mRNA levels were determined by quantitative real-time RT–PCR. Myocardial sections from HMGB1-Tg and WT mice were stained with anti-8-OHdG antibodies to evaluate the degree of DNA damage in the heart. The staining was visualized by treatment with a solution of 3,3′-diaminobenzidine (Dako Cytomation Liquid DAB Substrate Chromogen System, Dako Japan, Tokyo, Japan) for 40 s. 8-OHdG positive area was measured (five random fields to yield around 400 cardiomyocyte) using Image J software and expressed as fold increase over HMGB1-TG TAC mice. Results were normalized by arbitrarily setting the area of the 8-OHDG positive cells in HMGB1-TG TAC mice to 1.0. All experimental procedures were performed according to the animal welfare regulations of Yamagata University School of Medicine, and the study protocol was approved by the Animal Subjects Committee of Yamagata University School of Medicine. The investigation conformed to the Guide for the Care and Use of Laboratory Animals published by the US National Institutes of Health (NIH Publication, 8th Edition, 2011).

## 2.5 Co-immunoprecipitaton and immunoblotting

After samples were collected, protein extracts were prepared in modified radio-immunoprecipitation assay 1 (RIPA) buffer. Immunoprecipitation was performed with 1 μg of antibodies against acetyl-lysine or HMGB1 in 400 μg whole lysate protein or 150 μg nuclear protein. Normal rabbit or mouse IgG was used as a negative control. Lysates were incubated with anti-acetyl-lysine or HMGB1 overnight, and then incubated for 1 h with protein A/G-agarose beads. Samples were washed four times with buffer and subjected to western blot analysis.

## 2.6 Statistical analysis

Data are presented as means ± standard error of the mean (SEM). Differences between groups were evaluated using one-way analysis of variance with *post hoc* Bonferroni test. Survival curves after TAC were generated using the Kaplan–Meier method and compared using the log-rank test. A *P*-value $<0.05$ was considered statistically significant. Statistical analysis was performed with a standard statistical program package (JMP version 8; SAS Institute Inc., Cary, NC, USA).

# 3. Results

## 3.1 HMGB1 expression and localization in human failing hearts

To investigate the expression and localization of HMGB1 in human failing hearts, myocardial samples of patients with heart failure and healthy controls (*Table 1*) were analysed by immunohistochemistry. HMGB1 was

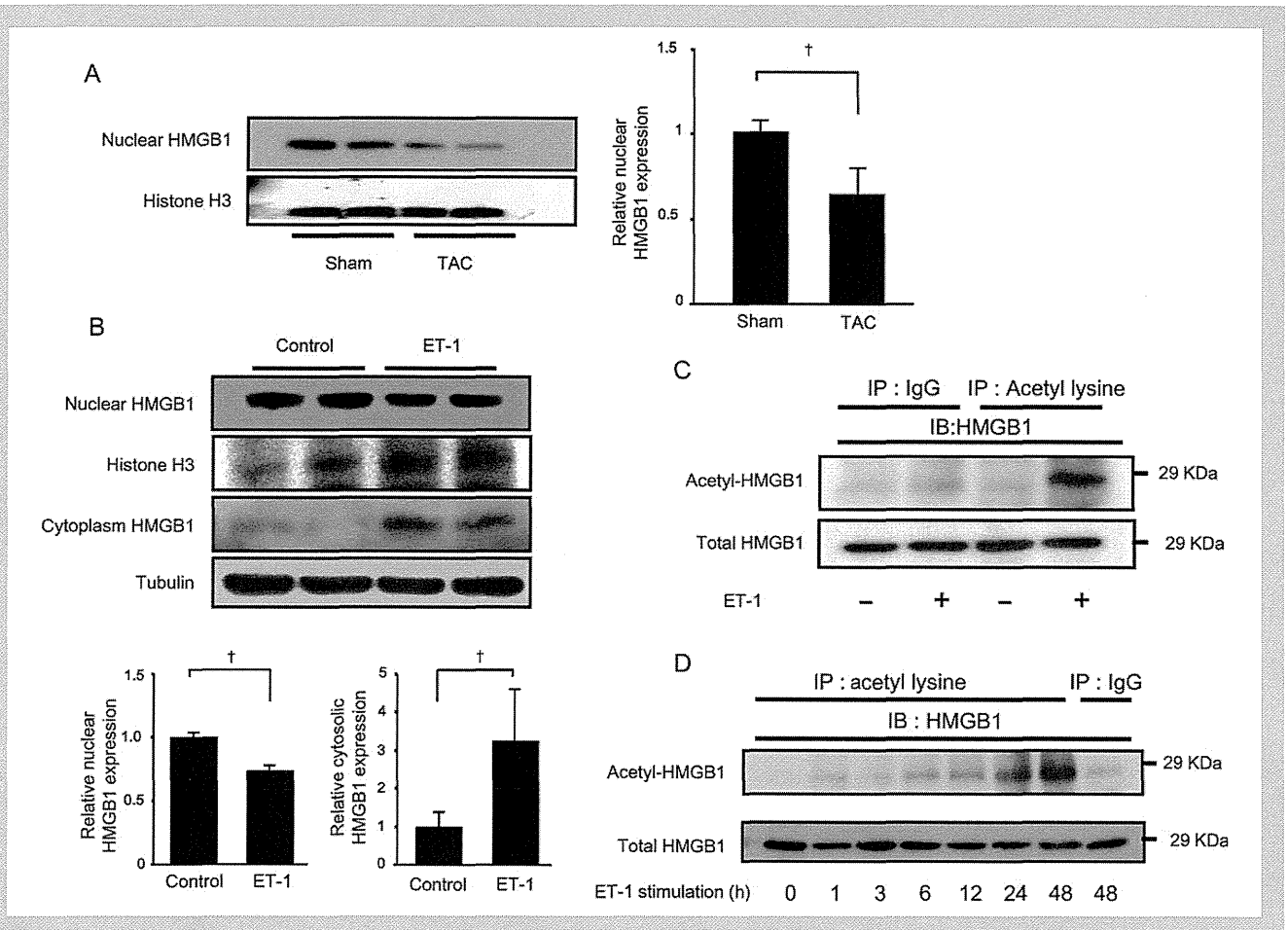


**Figure 2** Translocation of HMGB1 induced by pressure overload and hypertrophic stimulation. (*A*) Decrease in nuclear localization of HMGB1 after pressure overload. Data are expressed as means ± SEM. $^{\dagger}P < 0.05$ vs WT TAC mice. (*B*) HMGB1 expression in the nucleus and cytoplasm of neonatal rat cardiomyocytes after ET-1 (100 nM) stimulation. Data are expressed as means means ± SEM. $^{\dagger}P < 0.05$ vs control. (*C*) Lysates of neonatal rat cardiomyocytes treated with or without ET-1 were immunoprecipitated with an anti-acetyl-lysine antibody and immunoblotted against an anti-HMGB1 antibody. (*D*) Lysates of neonatal rat cardiomyocytes following stimulus with ET-1 (100 nM) were immunoprecipitated with an anti-acetyl-lysine antibody and immunoblotted against HMGB1.

localized in the nuclei of cardiomyocyte in control hearts (*Figure 1A*). On the contrary, decreased nuclear staining and increased cytosolic staining of HMGB1 were detected in the failing heart (*Figure 1B*). Comparison of the percentage of HMGB1 positively stained nuclei in failing and non-failing heart samples showed that nuclear HMGB1 expression was clearly lower in failing hearts than in control hearts (*Figure 1C*) because of the translocation of nuclear HMGB1 to the cytoplasm in failing hearts. These findings suggested that nuclear localization of HMGB1 in cardiomyocytes might be associated with cardiac dysfunction during cardiac remodelling.

## 3.2 Translocation and acetylation of HMGB1 induced by hypertrophic stimulation

To confirm whether translocation of HMGB1 was observed during LV remodelling, we evaluated the localization of HMGB1 in heart samples of mice in which pressure overload was generated by TAC. Similar to the observations in human failing heart samples, nuclear HMGB1 was decreased after TAC (*Figure 2A*). HMGB1 is mainly expressed in the nuclei of cardiomyocytes in sham mice. On the other hand, decreased nuclear staining and increased cytosolic staining of HMGB1 were observed in the cardiomyocytes after pressure overload (Supplementary material online, *Figure S1A* and *B*). However, HMGB1 expressions in endothelial cells were similar between sham- and TAC-operated mice (Supplementary material online, *Figure S1B*). Nuclear HMGB1 expression was decreased in neonatal rat cardiomyocytes after ET-1 (*Figure 2B*) or Ang II (Supplementary material online, *Figure S2A*) stimulation, whereas cytosolic HMGB1 was increased compared with without stimulation. To determine whether HMGB1 acetylation is associated with the localization of HMGB1 in cardiomyocytes, neonatal rat cardiomyocytes were stimulated with ET-1 or Ang II, and HMGB1 acetylation status was evaluated. ET-1 stimulation increased the acetylation of HMGB1, and in a time-dependent manner with a maximum at 48 h (*Figure 2C* and *D*). Ang II also induced HMGB1 acetylation as shown in Supplementary material online, *Figure S2B*. These findings indicated that nuclear HMGB1 translocated from the nucleus to the cytoplasm during cardiac remodelling.

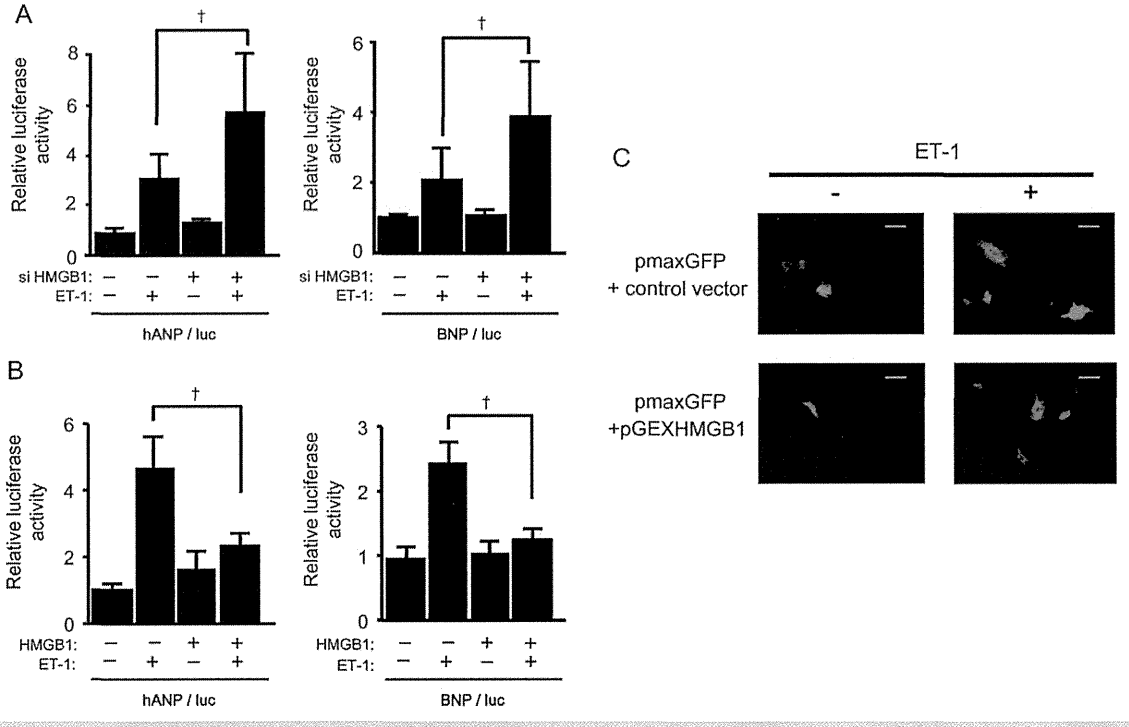


**Figure 3** Protective effect of nuclear HMGB1 on ET-1 induced hypertrophy. (*A*) Increase in ANP and BNP promoter activity by HMGB1 SiRNA transfection after ET-1 stimulation. Data represent means ± SEM from three independent experiments; $^{\dagger}P < 0.05$. (*B*) Suppressed ANP and BNP promoter activity after ET-1 stimulation in HMGB1 vector transfected cardiomyocytes. Data represent means ± SEM; $^{\dagger}P < 0.05$. (*C*) Effect of HMGB1 overexpression on the cell surface area of neonatal rat cardiomyocytes after ET-1 stimulation. Cardiomyocytes were transfected with pmax-GFP with either an HMGB1 expression vector or a control vector, and incubated for 48 h with or without ET-1. Scale bar = 20 μm.

## 3.3 The impact of nuclear HMGB1 on the cardiac foetal gene expression

To determine the impact of nuclear HMGB1 on cardiac hypertrophy, foetal cardiac gene expression in cardiomyocytes was assessed using HMGB1 siRNA. Specific siRNA against HMGB1 blocked its expression by >70% (Supplementary material online, *Figure S3A*). ANP and BNP promoter activities were increased by ET-1 stimulation in cardiomyocytes. Moreover, co-transfection with HMGB1 siRNA enhanced ANP and BNP promoter activities compared with control siRNA transfection (*Figure 3A*), and increased ANP RNA expression (Supplementary material online, *Figure S3B*), suggesting that loss of nuclear HMGB1 might be associated with cardiomyocyte hypertrophy during ET-1 stimulation.

To confirm whether the maintenance of HMGB1 levels in the nucleus could suppress the development of cardiomyocyte hypertrophy, the HMGB1 construct was co-transfected with ANP or BNP promoter luciferase constructs. Overexpression of HMGB1 significantly attenuated ANP and BNP promoter activity after ET-1 stimulation (*Figure 3B*). Similarly, the increase in ANP RNA expression after ET-1 stimulation was also suppressed by HMGB1 overexpression (Supplementary material online, *Figure S4A*). In addition, ET-1 induced hypertrophic changes in cardiomyocytes were significantly attenuated by HMGB1 overexpression (*Figure 3C*, Supplementary material online, *Figure S4B*). These findings implied that preservation of the expression of nuclear HMGB1 may suppress cardiomyocyte hypertrophy.

## 3.4 HMGB1 in the hypertrophic and heart failure model

To examine the role of nuclear HMGB1 in the development of cardiac hypertrophy and heart failure *in vivo*, cardiac-specific HMGB1 overexpressing (HMGB1-Tg) mice and WT mice were subjected to TAC or sham surgery. The levels of acetylated and cytosolic HMGB1 were similarly increased and cardiac nuclear HMGB1 was decreased after TAC in WT and HMGB1-Tg mice compared with those undergoing sham surgery (*Figure 4A*). Notably, nuclear HMGB1 levels after TAC were higher in HMGB1-Tg mice than in WT mice, indicating that nuclear HMGB1 levels were preserved in HMGB1-Tg mice (*Figure 4A*). To investigate the role of nuclear HMGB1 in protecting cardiomyocytes from DNA damage in cardiac hypertrophy, we performed immunohistochemical staining of TAC-operated hearts using an anti- 8-OHdG antibody (*Figure 4B*). Sham-operated mice did not show 8-OHdG positive cardiomyocytes. On the other hand, in mice undergoing TAC, 8-OHdG expression was significantly increased in both HMTG1-TG and WT mice, whereas the induction of 8-OHdG was suppressed in HMGB1-Tg mice. Comparison of the relative 8-OHDG positively stained cells in WT and Tg mice after TAC showed that 8-OHDG expression was clearly lower in Tg mice than in WT mice (*Figure 4C*).

At 4 weeks after the TAC operation, the increase in the weight of the heart was significantly lower in HMGB1-Tg mice than in WT-mice (*Figure 5A*). We next examined the mRNA expression of foetal cardiac

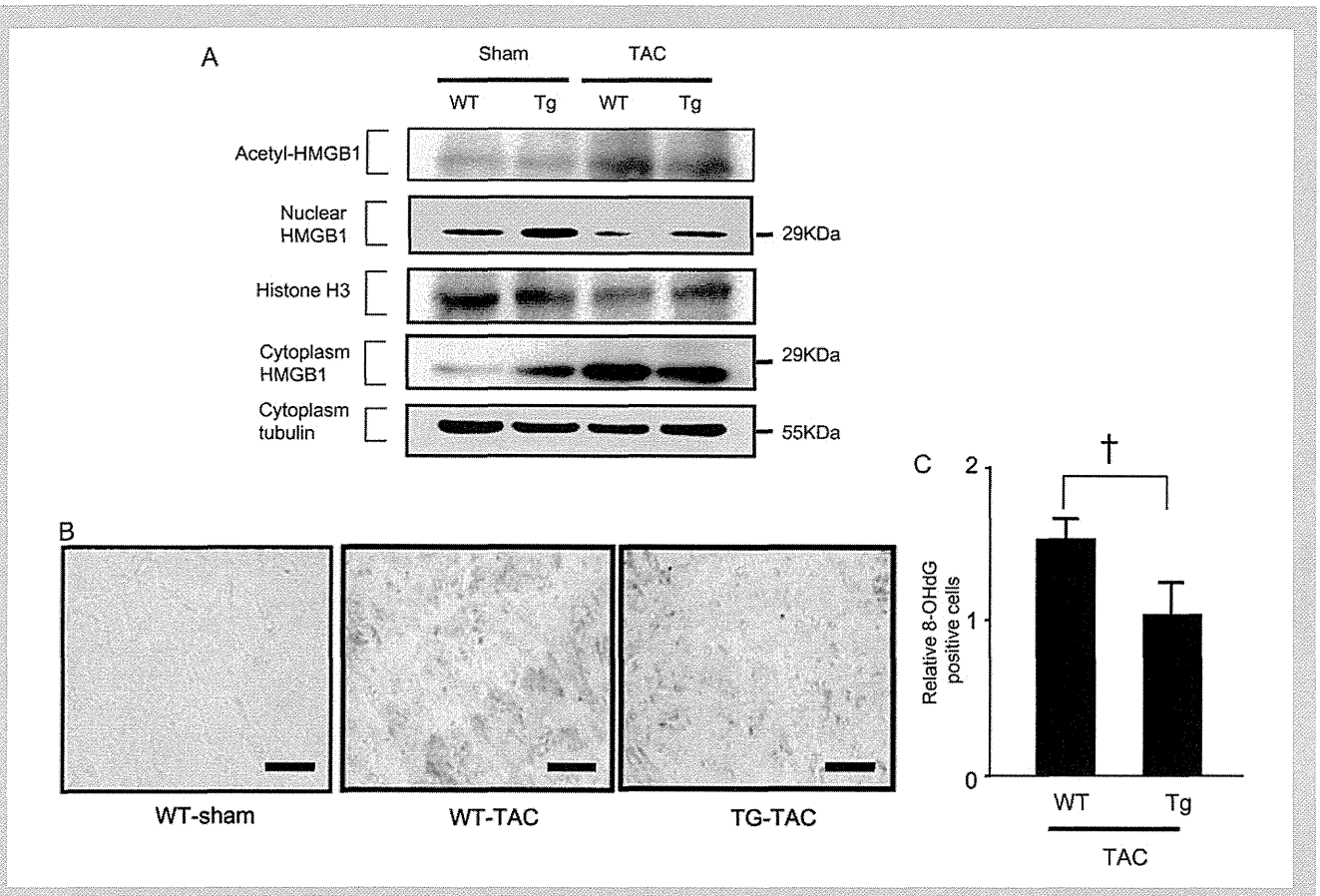


**Figure 4** Preserved amounts of nuclear HMGB1 prevented DNA damage induced by pressure overload. (*A*) Acetylation and translocation of cardiac HMGB1 from the nucleus to the cytoplasm after pressure overload. (*B*) Immunohistochemical staining of heart tissues with an anti-8-OHdG antibody 4 weeks after TAC and quantification of histological data ($n = 5$). Scale bar, 50 mm. (*C*) Results were normalized by arbitrarily setting the area of the 8-OHDG positive cells in HMGB1-TG TAC mice to 1.0. Bars represent means ± SEM. ($n = 5$). $^{\dagger}P < 0.05$ vs. WT TAC mice.

genes after TAC. The expressions of ANP, BNP, and β-MHC were significantly up-regulated in the TAC group compared with the sham-surgery group, and this up-regulation was significantly attenuated in HMGB1-Tg mice (*Figure 5B*). Moreover, systolic dysfunction and left-ventricular dilatation after TAC were attenuated in HMGB1-Tg mice compared with WT-mice (*Figure 5C*, Supplementary material online, *Table*). Furthermore, the survival rate after TAC was significantly higher in HMGB1-Tg mice than in WT mice (*Figure 5D*).

## 4. Discussion

In the present study, we demonstrated the critical role of intracellular HMGB1 in the development of cardiac hypertrophy and heart failure. We found that cardiac HMGB1 was exported from the nucleus to the cytoplasm in patients with heart failure. Our *in vitro* study showed that nuclear HMGB1 was acetylated and translocated to the cytoplasm in neonatal rat cardiomyocytes in response to ET-1 and Ang II stimulation. We also demonstrated that loss of nuclear HMGB1 aggravated foetal gene expressions induced by ET-1 stimulation. In contrast, this up-regulation of gene expression was suppressed by HMGB1 overexpression. We further showed that preserved HMGB1 expression in the nucleus attenuated DNA damage during pressure overload, and abolished ventricular remodelling and cardiac dysfunction.

HMGB1, which is ubiquitously expressed in all vertebrate nuclei with a uniquely conserved sequence among species, was identified as a chromosomal protein with important structural functions in chromatin organization.[5,6] HMGB1 binds to double-stranded DNA and interacts with other DNA-binding proteins, which facilitate chromatin bending.[28,29] On the other hand, HMGB1 released or secreted into the circulation has attracted attention for its cytokine-like function and involvement in the pathology of cardiovascular disease.[8,12,30,31] Scaffidi *et al.*[8] reported that HMGB1 secreted from inflammatory cells and passively released from necrotic cells promoted inflammation. A role for extracellular HMGB1 in the regulation of inflammation was proposed based on its association with Toll-like receptor family members, the interleukin-1 receptor, and the receptor for advanced glycation end-products.[10,16,32,33] However, the localization of HMGB1 in cardiomyocytes and its potential role in the pathogenesis of human heart failure have not been studied in detail. In the present study, HMGB1 localized to the nucleus in the non-failing heart, as expected, whereas nuclear HMGB1 levels decreased and cytosolic HMGB1 increased in the failing human heart. These findings suggest that nuclear HMGB1 may play an important role in the regulation of cardiomyocyte phenotype in relation to the pathogenesis of human heart failure.

In addition to the mechanisms mediating the secretion of HMGB1 from necrotic cells, other pathways involved in the export of HMGB1